AGU PUBLICATIONS

Tectonics

RESEARCH ARTICLE
10.1002/2017TC004611

**Key Points:**
- Zircon geochronology and geochemistry indicate an extensional arc system within the Antarctic sector of the Gondwana margin
- The extensional arc system in the Antarctic sector is a continuation of the extensional arc system in the adjacent Australian sector
- An along-arc switch to advancing arc tectonics in South America is located in the vicinity of the Thurston Island block of West Antarctica

**Supporting Information:**
- Supporting Information S1
- Data Set S1
- Data Set S2

**Correspondence to:**
D. A. Nelson,
demian@umail.ucsb.edu

**Citation:**
Nelson, D. A., & Cottle, J. M. (2017). Long-term geochemical and geodynamic segmentation of the paleo-Pacific margin of Gondwana: Insight from the Antarctic and adjacent sectors. *Tectonics*, *36*, 3229–3247. https://doi.org/10.1002/2017TC004611

Received 7 APR 2017
Accepted 14 NOV 2017
Accepted article online 23 NOV 2017
Published online 22 DEC 2017
Corrected 6 FEB 2018

This article was corrected on 6 FEB 2018. See the end of the full text for details.



# Long-Term Geochemical and Geodynamic Segmentation of the Paleo-Pacific Margin of Gondwana: Insight From the Antarctic and Adjacent Sectors

**D. A. Nelson**[1] and **J. M. Cottle**[1]

[1]Department of Earth Science, University of California, Santa Barbara, CA, USA

**Abstract** Combined zircon geochemistry and geochronology of Mesozoic volcaniclastic sediments of the central Transantarctic Mountains, Antarctica, yield a comprehensive record of both the timing and geochemical evolution of the magmatic arc along the Antarctic sector of the paleo-Pacific margin of Gondwana. Zircon age populations at 266–183 Ma, 367–328 Ma, and 550–490 Ma correspond to episodic arc activity from the Ediacaran to the Jurassic. Zircon trace element geochemistry indicates a temporal shift from granitoid-dominated source(s) during Ediacaran to Early Ordovician times to mafic sources in the Devonian through Early Jurassic. Zircon initial $\varepsilon_{Hf}$ shifts to more radiogenic Hf isotope compositions following the Ross Orogeny and is inferred to reflect juvenile crustal growth within an extensional arc system during progressive slab rollback. These new ages and Hf isotopic record are similar to those from the Australian sector, indicating that these regions constituted an ~3,000 km laterally continuous extensional arc from at least the Carboniferous to the Permian. Conversely, the South American sector records enriched zircon Hf isotopic compositions and compressional/advancing arc tectonics during the same time period. Our new data constrain the location of this profound along-arc geochemical and geodynamic "switch" to the vicinity of the Thurston Island block of West Antarctica.

## 1. Introduction

The paleo-Pacific margin of Gondwana (Figure 1a) was a relatively continuous active convergent margin from at least the Ediacaran until initial supercontinent breakup in the Early Jurassic (Cawood, 2005; Collins et al., 2011). The volcanic, plutonic, metamorphic, and sedimentary products of this protracted convergence are found within various allocthonous, autocthonous, and para-autocthonous terranes throughout Peru, Chile, Antarctica, New Zealand, and Australia (Figure 1a). Recent work has significantly improved our knowledge of this major arc system, primarily through detrital and igneous zircon geochronology and geochemistry of rocks from South America and Australia (e.g., Cawood et al., 2011; Kemp et al., 2009; Pepper et al., 2016). However, the segment of the post-Ordovician arc system within the Antarctic sector (Figure 1b), that is, the various crustal blocks of Zealandia and particularly West Antarctica, remains poorly understood due to a lack of data, largely a result of poor exposure and/or inaccessibility (i.e., ice covered or submarine continental crust). Unraveling the history of this segment of the arc is further complicated by a lack of robust paleomagnetic constraints on the relative locations and relationships between crustal blocks of West Antarctica and Zealandia from their presumed initial formation in the Neoproterozoic to Cambrian through to their breakup in the Cretaceous. In addition, extensive rifting, rotation, and translation of these crustal blocks since the Cretaceous means that this segment of the arc is highly dissected and makes reconstructing the prebreakup configuration of the paleo-Pacific margin of Gondwana a difficult task (Dalziel & Elliot, 1982; Grunow et al., 1987; Storey et al., 1988) and has resulted in a gap in the record of the broad history of the paleo-Pacific margin of Gondwana.

A comprehensive archive of post-Ordovician arc volcanism along the Antarctic sector is recorded in Mesozoic volcaniclastic sediments deposited in a foreland basin setting that is now exposed in the Transantarctic Mountains (TAM; Barrett et al., 1986, Figure 2). In contrast to West Antarctica and Zealandia, which have undergone large-scale translation and rotation, sediments in the TAM were deposited onto a section of the East Antarctic craton that remained tectonically undissected during supercontinent breakup. The Mesozoic strata studied here, the Fremouw and Hanson Formations, therefore provide an opportunity to characterize the evolution of the segment of the arc outboard of the TAM without the need for extensive paleogeographic reconstructions and associated uncertainties. The source(s) outboard of the TAM for

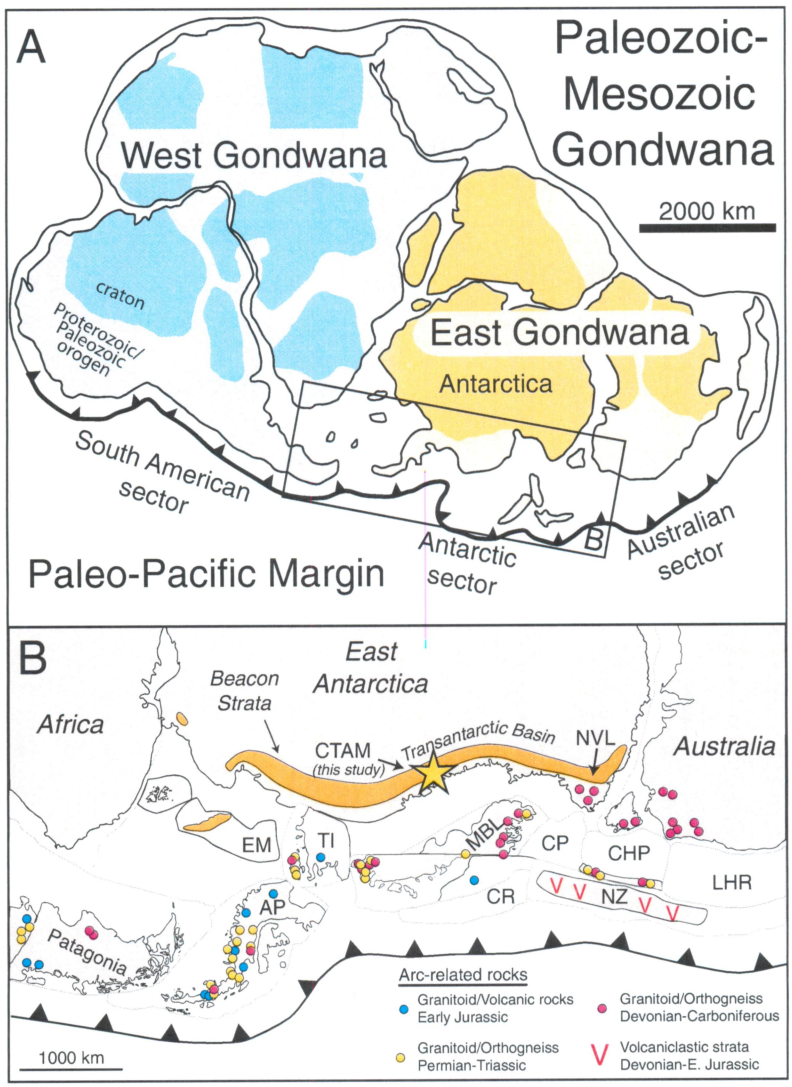


**Figure 1.** (a) Paleogeographic reconstruction of supercontinent Gondwana during the Paleozoic-Mesozoic and the major sectors of the active paleo-Pacific margin of Gondwana (modified from Meert & Lieberman, 2008). (b) Reconstruction of the Antarctic sector of the Gondwana plate margin during the late Paleozoic–early Mesozoic, showing the location of the study area in the cTAM relative to the distribution of Devonian through early Jurassic arc-related rocks located within the various outboard crustal blocks (Elliot, 2013). West Antarctica: EM, Ellsworth Whitmore; TI, Thurston Island; AP, Antarctic Peninsula; MBL, Marie Byrd Land. Zealandia: CR, Chatham rise; CP, Cambell Plateau; NZ, East New Zealand; LHR, Lord Howe rise; CHP, Challenger Plateau and West New Zealand.

volcanic detritus in these formations is presumed to be located in Zealandia, West Antarctica, and/or Patagonia (Elliot et al., 2017; Elliot, Fanning, et al., 2016; Elliot, Larsen, et al., 2016; Elsner et al., 2013; Fanning et al., 2011). This contribution presents the first study that combines zircon U-Pb geochronology, trace elements, and Hf isotopes for volcaniclastic sediments in the TAM in order to determine major periods of arc volcanism and the relative roles of crustal growth and recycling, and reconstruct the large-scale tectonic history of the Antarctic sector arc of the Gondwana margin. These data are further interrogated alongside data from other portions of the margin to infer the geodynamic and mantle evolution of the Antarctic sector relative to the South American and Australian sectors.

## 2. Geologic Background

Volcaniclastic sedimentary rocks of the Hanson and Fremouw Formations are among the youngest rocks (the Victoria Group) of the Devonian to Lower Jurassic strata of the Beacon Supergroup found throughout the

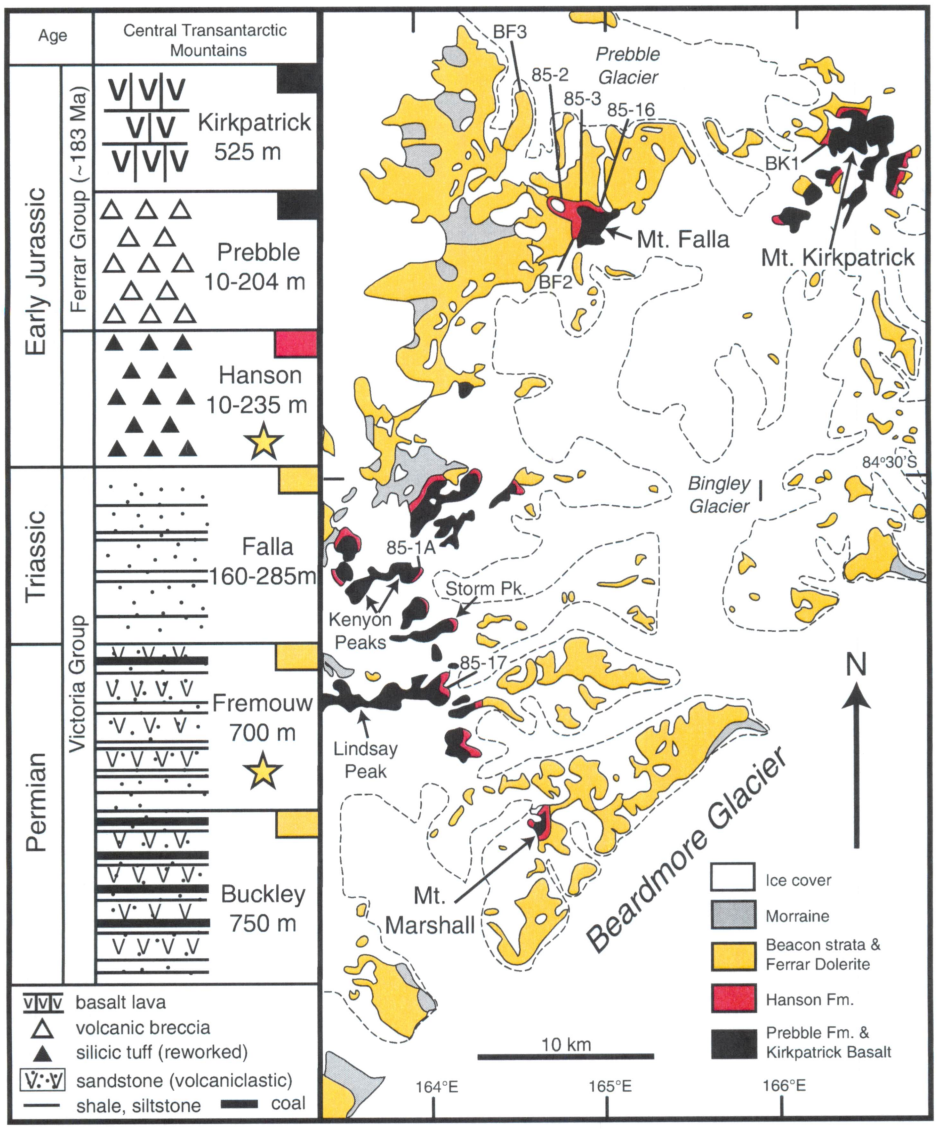


**Figure 2.** Simplified geologic map of the cTAM and a generalized stratigraphic column. Letters and/or numbers refer to the original collector's sampling locations and measured stratigraphic columns (modified from Elliot, Fanning, et al., 2016; Elliot, Larsen, et al., 2016). Shenk Peak, Mount Rosenwald, and Mount Black are out of the map area.

TAM (Figure 2). The Beacon Supergroup was deposited in the Transantarctic Basin that extends roughly the length of the TAM and formed between the stable East Antarctic Craton and the active magmatic arc of the paleo-Pacific Gondwana margin (Collinson et al., 1994). The oldest sediments of the Beacon Supergroup, the Taylor Group, are separated uncomformably from the crystalline basement (Granite Harbor Intrusives, GHI, Gunn & Warren, 1962) of the Neoproterozoic to Ordovician Ross Orogen by the Kukri Erosion Surface (LeMasurier & Landis, 1996). Pre-Ross age igneous rocks in the TAM are limited to Proterozoic to Mesoarchean orthogneisses exposed in the Miller Range (central TAM, cTAM) (Goodge & Fanning, 2016).

The GHI of the Ross Orogen were emplaced between circa 590–485 Ma (Cox et al., 2000; Goodge et al., 2012; Hagen-Peter et al., 2015; Paulsen et al., 2013) and represent initiation of arc magmatism along the Antarctic sector of the paleo-Pacific margin of Gondwana in the Ediacaran (Walker et al., 2013). The Delamarian Orogen in Australia contains correlative rocks to the Ross Orogen, both of which are components of the larger Terra-Australis Orogen (Cawood, 2005; Foden et al., 2006). Isolated examples of Ross-Delamerian-aged

rocks also occur in West Antarctica and Zealandia (Allibone et al., 2009; Gibson & Ireland, 1996; Mukasa & Dalziel, 2000; Pankhurst & Weaver, 1998).

Following the termination of the Ross Orogeny in the Ordovician, the magmatic arc migrated outboard into West Antarctica, the Antarctic Peninsula, and Zealandia (summarized in Elliot, 2013). During this time the Transantarctic basin developed behind the arc and evolved from a back-arc basin in the Early Permian to a foreland basin during the Gondwanide Orogeny in the Late Permian-Triassic times (Collinson et al., 1994). Major influxes of volcanic detritus into the Transantarcic basin occurred in the late Early Permian with accumulation continuing through the Early Jurassic (Elliot et al., 2017; Elliot, Fanning, et al., 2016; Elliot, Larsen, et al., 2016). Volcanic and magmatic rocks similar in age to the volcanic detritus in the Transantarctic basin occur in Zealandia, West Antarctica, the Antarctic Peninsula, and Patagonia (summarized in Elliot, 2013). For this reason, workers have variously attributed the source of the TAM volcanic detritus to contemporary arc volcanism in one or more of these regions (Elliot & Fanning, 2008; Elliot et al., 2017; Elliot, Fanning, et al., 2016; Elliot, Larsen, et al., 2016; Elsner et al., 2013; Fanning et al., 2011). However, correlations between the volcaniclastic sedimentary rocks of the Hanson and Fremouw Formations and their potential source region(s) rely chiefly on geochronology rather than a combination of geochronology and complimentary isotopic and elemental tracer data for unaltered/unmodified volcaniclastic sediments or minerals (i.e., zircon). Consequently, previous detrital zircon studies in the TAM have not been able to better constrain the igneous source regions nor derive an unambiguous record of the geochemical evolution of the arc through time.

### 2.1. Hanson and Fremouw Formations

Well-exposed sections of Triassic to Jurassic Beacon Supergroup strata in the central TAM (cTAM) contain fluvial sediments of the Triassic Fremouw Formation (Figure 2; Collinson et al., 1994; Elliot & Fanning, 2008). Variable amounts of volcanic detritus throughout the Fremouw Formation and the underlying Buckley Formation are inferred to record contemporaneous volcanism sourced from the outboard magmatic arc (Barrett et al., 1986; Elliot & Fanning, 2008). Recent zircon geochronology for the Fremouw Formation provide early Triassic maximum deposition ages of 245.9 ± 2.9 Ma and 242.3 ± 2.3 Ma, improving the record of contemporaneous volcanism (Elliot et al., 2017).

Overlying the Fremouw Formation is the Late Triassic Falla Formation and the Early Jurassic volcaniclastic-rich Hanson Formation. The Hanson Formation consists of tuffs, tuffaceous sandstones, arkosic grits and sandstones, and lapillistones that comprise a 235 m thick section at the type locality at Mount Falla (Figure 2; Elliot, 1996; Elliot, Fanning, et al., 2016; Elliot, Larsen, et al., 2016). The only other section of correlative Early Jurassic reworked silicic tuffs with exposed upper and lower contacts, the Shafer Peak Formation, occurs in the Deep Freeze Range in northern Victoria Land (NVL, Figure 1b; Schöner et al., 2007; Elsner et al., 2013). Tuffs of the Hanson Formation are dacitic to rhyolitic in composition (~67 to 78 wt % $SiO_2$) with the majority containing evidence for fluvial reworking, with relatively few primary tuffs that, where present, are interpreted to represent unmodified airfall deposits resulting from distal (super)plinian eruptions (Elliot, 2000; Elliot et al., 2007; Elliot, Fanning, et al., 2016; Elliot, Larsen, et al., 2016). Whole-rock geochemistry and Ar-Ar geochronology are compromised by admixed detrital material and zeolite alteration (Elliot et al., 2007). However, whole rock major and trace elements and Sr and Nd isotopic data for the least modified tuffs suggest derivation from a volcanic arc (Elliot, Fanning, et al., 2016; Elliot, Larsen, et al., 2016).

The Hanson and Shafer Peak Formations are designated Early Jurassic in age because they are younger than the Upper Triassic Dicroidium-bearing sandstones of the underlying Falla (cTAM) and Section Peak (NVL) Formations and are overlain by the ~182.8 Ma Kirkpatrick lavas and pyroclastics of the Prebble and Exposure Hill Formations (Figure 2; Burgess et al., 2015). An early Jurassic age for tuffs of the Hanson Formation is supported by U-Pb zircon ages of 182.7 ± 1.8 Ma, 186.2 ± 1.7 Ma, and 194.0 ± 1.6 Ma (Elliot et al., 2007; Elliot, Fanning, et al., 2016; Elliot, Larsen, et al., 2016). These age constraints indicate that Hanson tuff deposition continued up to, and was perhaps contemporaneous with, emplacement of mafic sills and lavas of the Early Jurassic Ferrar Large Igneous Province (LIP) that forms a 3,500 km linear belt along the TAM (Burgess et al., 2015; Elliot & Fleming, 2004). However, the tectonomagmatic relationship between Early Jurassic volcanism as preserved in the Hanson Formation and the Ferrar LIP magmatism remains unknown (Elliot et al., 2007). U-Pb detrital zircon dates from Shafer Peak and Section Peak formations provide maximum deposition ages spanning from ~190 Ma to the Upper Triassic (Elsner et al., 2013). All of these formations also

contain significant proportions of principally Ediacaran to Ordovician and late Mesoproterozoic to early Neoproterozoic detrital zircon, that is, a typical "Gondwana signature," inferred to originate from erosion of proximal crystalline basement and/or lower Paleozoic strata or recycling from underlying strata or from similar aged rocks outboard in West Antarctica and Zealandia (Elliot et al., 2015; Elliot et al., 2017; Elliot, Larsen, et al., 2016).

### 2.2. Potential Volcanic Sources

Numerous examples of Paleozoic-Mesozoic magmatic and volcanic potential source rocks have been discovered throughout the paleo-Pacific margin of Gondwana (Figure 1b; Elliot, 2013). However, notwithstanding complications from contamination and/or alteration of isotopic ratios by detrital components and zeolite alteration Elliot et al. (2007), Elliot, Fanning, et al. (2016), and Elliot, Larsen, et al. (2016) suggested that dissimilar whole-rock Sr and Nd isotopic compositions of available Mesozoic West Antarctic magmatic rocks indicate that they are not a direct source for the Early Jurassic Hanson Formations. Despite a lack of isotopic data, Permian and Triassic arc-related rocks within West Antarctica and Patagonia have also been suggested to represent potential source regions for Permian-Triassic volcaniclastic units in the cTAM (Elliot et al., 2017; Fanning et al., 2011).

Potential sources also exist in Zealandia, where both *in situ* magmatic rocks and detrital zircons record arc activity throughout the Mesozoic and earlier (Figure 1b; Elliot, 2013; Kimbrough et al., 1994; Adams et al., 2002; Adams, Korsch, & Griffin, 2013; Elliot, 2013; Kimbrough et al., 1994; Mortimer et al., 2015). Nevertheless, unexposed/undiscovered magmatic rocks in West Antarctica (e.g., Marie Byrd Land) remain the prevailing volcanic source region hypothesis for volcanic detritus material in the cTAM Beacon Supergroup (Elliot et al., 2017; Elliot, Fanning, et al., 2016; Elliot, Larsen, et al., 2016; Elsner et al., 2013).

## 3. Sampling and Methods

This study presents zircon geochronology and geochemistry from 25 rock samples of the Hanson Formation and 5 rock samples of the Fremouw Formation selected from the Polar Rock Repository (doi:10.7289/V5RF5S18) representing various stratigraphic heights and sections in the cTAM (see Figure S1 in the supporting information). Zircons were separated using standard mineral separation techniques (i.e., disk milling, water table, magnetic separation, and heavy liquids). Representative zircon from each sample were mounted in epoxy and polished to expose equatorial sections. Prior to isotopic analysis, zircons were imaged via cathodoluminescence on an FEI Quanta400f scanning electron microscope and used to guide selection of locations for laser ablation split-stream (LASS) (U-Pb and trace elements) and Lu-Hf measurements.

Zircon U-Pb isotopes and trace element concentrations were obtained simultaneously using the "split stream" approach (Kylander-Clark et al., 2013) at the University of California, Santa Barbara, under standard operating conditions (McKinney et al., 2015). Instrumentation consists of a 193 nm ArF excimer laser ablation (LA) system coupled to Nu Plasma high-resolution multicollector-inductively coupled plasma mass spectrometer (MC-ICP-MS) for U/Pb and a Agilent 7700S Quadrupole ICP-MS for trace elements. Between 60 and 100 grains were measured for U-Pb and trace element analysis from each sample. Subsequent Lu-Hf analyses were performed by LA-MC-ICP-MS exclusively on zircon younger than Ordovician ($n$ = 15 per sample) to better characterize the geochemistry of post-Ross-aged zircon. All data reduction was performed using Iolite v2.5 (Paton et al., 2011, 2010), and $^{207}$Pb-corrected $^{206}$Pb/$^{238}$U ages were calculated for zircon younger than circa 800 Ma using the method of Andersen (2002) and ISOPLOT/EX (Ludwig, 2003). Detailed analytical methods, data reduction protocols, and results of reference zircon analyses and unknown data are provided in the supporting information Text S1 and Data Sets S1 and S2 (Blichert-Toft, 2008; Chu et al., 2002; Jackson et al., 2004; Liu et al., 2010; Patchett & Tatsumoto, 1980, 1981; Sláma et al., 2008; Thirlwall & Anczkiewicz, 2004; Wiedenbeck et al., 1995, 2004; Woodhead & Hergt, 2005).

## 4. Results

### 4.1. Geochronology

Twenty-two of the 25 samples of the Hanson Formation and all samples of the Fremouw Formation contain zircon age populations near the inferred stratigraphic age of the sample and allow for determination of maximum deposition ages (summarized in Table 1). In addition, populations of older detrital zircon are

**Table 1**
*Summary of Maximum Deposition Ages From Zircon U-Pb Geochronology*

| | PRR# | Location | Maximum deposition age (Ma) | Mean square weighted deviation | $n$ ($n$ < 250 Ma) | Rejected | $n$ (> 205 Ma) | % detrital |
|---|---|---|---|---|---|---|---|---|
| Hanson Formation | | | | | | | | |
| | PRR-26916 | Kenyon Peaks | 189.3 ± 0.7 | 1.3 | 71 | 13 | 15 | 15 |
| | PRR-26917 | Kenyon Peaks | 184.9 ± 1.3 | 1.4 | 20 | 5 | 36 | 59 |
| | PRR-26932 | Mt. Falla | 197.4 ± 1.1 | 1.6 | 19 | 0 | 41 | 68 |
| | PRR-26934 | Mt. Falla | 199.5 ± 0.7 | 1 | 75 | 0 | 13 | 15 |
| | PRR-26943 | Mt. Falla | n.d | | 23 | | 24 | 51 |
| | PRR-26949 | Mt. Falla | 195.1 ± 0.6 | 1 | 53 | 10 | 24 | 28 |
| | PRR-26951 | Mt. Falla | 188.0 ± 0.9 | 0.7 | 24 | 7 | 46 | 60 |
| | PRR-26960 | Mt. Falla | 187.8 ± 0.7 | 0.9 | 32 | 1 | 31 | 48 |
| | PRR-26968 | Mt. Falla | 193.5 ± 0.7 | 0.7 | 45 | 12 | 27 | 32 |
| | PRR-26979 | Mt. Falla | 189.5 ± 2.4 | 2.5 | 16 | 8 | 40 | 63 |
| | PRR-26981 | Mt. Falla | 189.3 ± 3.2 | 1.8 | 7 | 0 | 83 | 92 |
| | PRR-26982 | Mt. Falla | n.d | | 7 | | 49 | 88 |
| | PRR-27068 | Mt. Petlock | 191.1 ± 0.8 | 1.2 | 40 | 13 | 38 | 42 |
| | PRR-27084 | Mt. Falla | 193.1 ± 1.1 | 1.1 | 29 | 9 | 23 | 38 |
| | PRR-27089 | Mt. Falla | 189.4 ± 0.7 | 1.6 | 52 | 7 | 11 | 16 |
| | PRR-27102 | Storm Peak | 194.4 ± 1.0 | 0.6 | 46 | 20 | 26 | 28 |
| | PRR-27112 | Storm Peak | 190.0 ± 0.8 | 1 | 36 | 9 | 27 | 38 |
| | PRR-27184 | Mt. Falla | n.d | | | | 71 | 100 |
| | PRR-27252 | Mt. Falla | 191.0 ± 2.1 | 0.5 | 8 | 2 | 86 | 90 |
| | PRR-05127 | Mt. Kirkpatrick | 190.8 ± 0.6 | 0.8 | 45 | 5 | 6 | 11 |
| | PRR-05493 | Mt. Falla | 187.9 ± 0.9 | 1.5 | 36 | 4 | 28 | 41 |
| | PRR-34456 | Mt. Falla | 193.4 ± 1.3 | 2.2 | 31 | 11 | 17 | 29 |
| Fremouw Formation | | | | | | | | |
| | PRR-26024 | Shenk Peak | 244.7 ± 1.7 | 0.8 | 22 | 13 | 26 | 43 |
| | PRR-25978 | Mt. Rosenwald | 242.8 ± 1.7 | 1.2 | 17 | 10 | 6 | 18 |
| | PRR-25968 | Mt. Rosenwald | 241.2 ± 1.5 | 0.4 | 52 | 44 | 5 | 5 |
| | PRR-26040 | Mt. Black | 247.9 ± 1.7 | 1.1 | 16 | 8 | 47 | 66 |
| | PRR-05099 | Mt. Kirkpatrick | 242.7 ± 2.9 | 1.9 | 16 | 9 | 29 | 54 |

also present (representative examples are plotted in Figure 3). To compute maximum depositional ages, Kernel Density estimates (KDE; Vermeesch, 2012) were constructed for each sample using only zircon near the stratigraphic age of the formation (i.e., zircon <205 Ma for the Hanson Formation and <260 Ma for the Fremouw Formation), and a subset of the youngest of those dates was used to calculate a weighted mean age (Figure 3). Overall, maximum deposition ages young upward, consistent with the stratigraphic relationships, and range from 199.5 ± 0.7 to 184.9 ± 1.3 Ma for the Hanson Formation and 247.9 ± 1.7 to 241.2 ± 1.3 Ma for the Fremouw Formation. These ages support an Early Jurassic depositional age for the Hanson Formation and an Early to Middle Triassic age for the Fremouw Formation (Figure S1; Collinson & Elliot, 1984; Elliot et al., 2017; Elliot, Larsen, et al., 2016).

The remaining zircon in each sample (> 205 Ma in the Hanson Formation and >260 Ma in the Fremouw) make up a considerable proportion of the total data, ranging from ~17 to 68% of measured zircon in each sample (Figure 3). To enable direct comparison among all data, zircon in the Hanson Formation and Fremouw Formation are compiled and illustrated on a single KDE (Figure 4). The most abundant zircon subpopulations in both formations are those near the formation's stratigraphic age. The Hanson Formation, however, also contains a continuous range of zircon ages from the Early Jurassic to the Late Permian as well as a minor Devonian-Carboniferous population. Similarly, the Fremouw Formation contains an overlapping Permo-Triassic subpopulation but a more abundant Devonian-Carboniferous subpopulation than samples of the Hanson Formation. Combined, the Hanson and Fremouw formations contain zircon ages ranging from 266 to 183 Ma and 367 to 328 Ma (Figure 4) In addition, approximately one quarter of all analyzed zircon from both formations are Ordovician or older and collectively represent a typical Gondwana signature, characterized by a peak between 550 and 490 Ma (corresponding to the

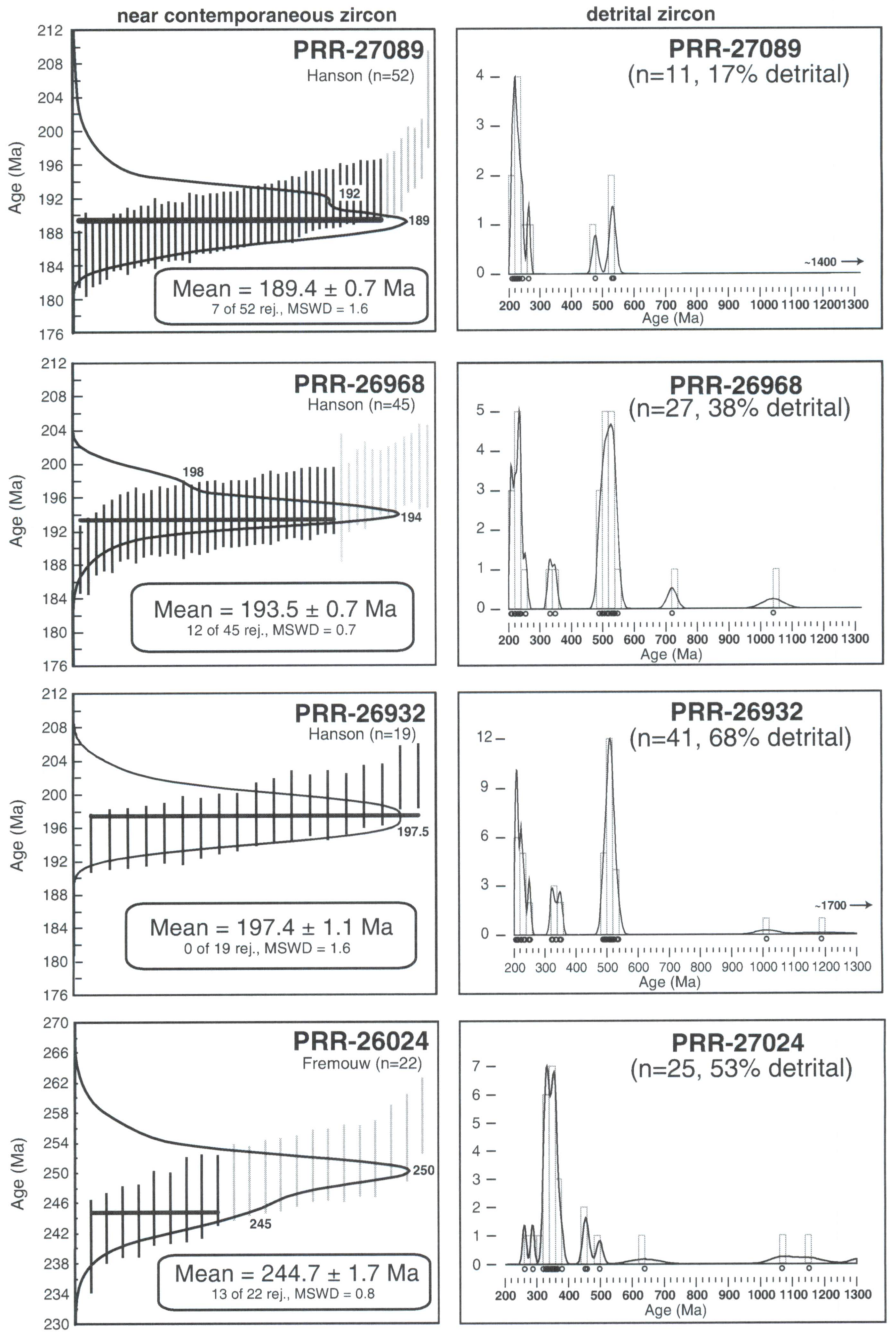


**Figure 3.** Zircon LASS U-Pb geochronology data for representative samples of the Hanson and Fremouw formations. (left column) Calculated weighted mean $^{207}Pb$-corrected $^{206}Pb/^{238}U$ maximum deposition ages for near-contemporaneous zircon (see text for explanation). (right column) Kernel density estimate (KDE) plot for detrital zircon of the same sample from the left column. See Data Set S1 for full U-Pb data set.

Ross-Delamarian Orogeny), a peak between 1,210 and 1,000 Ma (corresponding to the Grenville Orogeny), and a minor component older than 1.3 Ga (not shown).

### 4.2. Trace Elements

Zircon trace element data are provided in Data Set S1 and discriminatory trace elements and ratios, that is, Hf ppm and Th/U are plotted in Figure 5. The "short" classification and regression tree (CART) were applied to

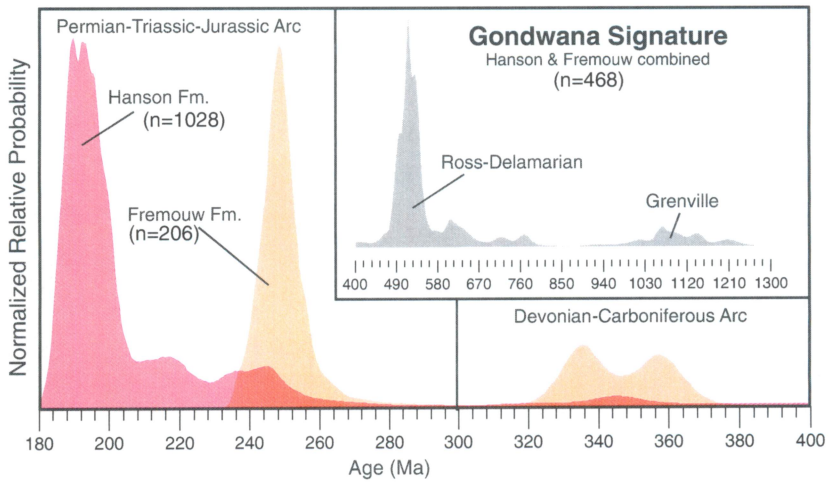


**Figure 4.** Kernel density estimate summarizing all zircon U-Pb geochronology data from this study. Devonian and younger zircon ages are grouped according to formation, and all older ages are combined. Zircon ages >1,300 Ma have been omitted. See Data Set S1 for full U-Pb data set.

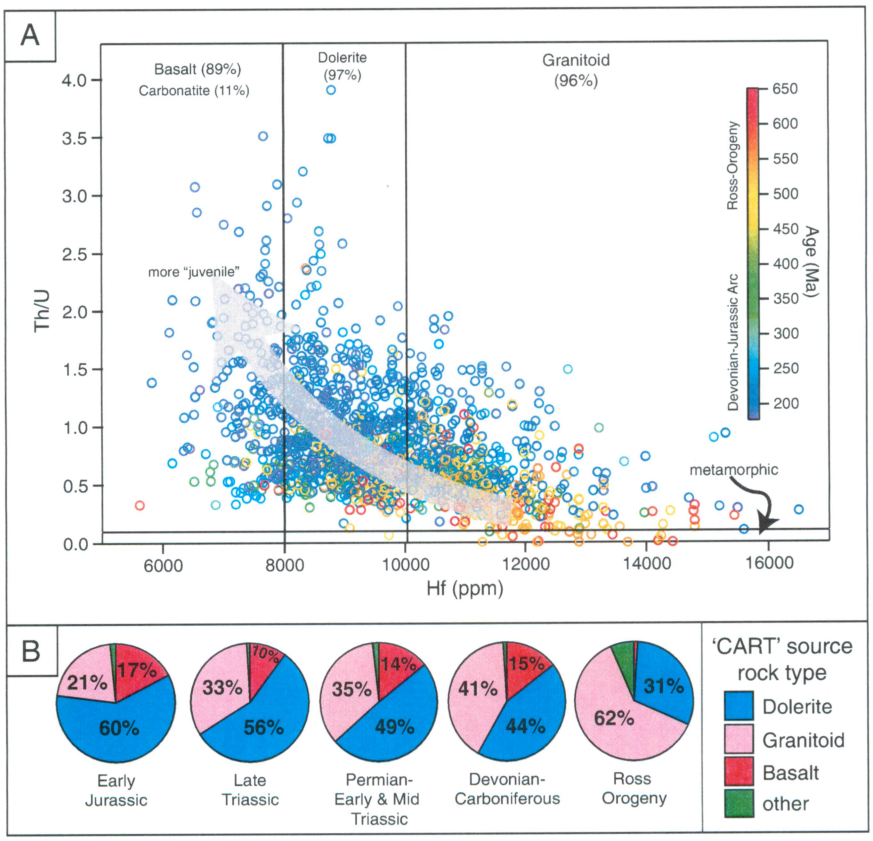


**Figure 5.** (a) Plot of zircon Hf ppm versus zircon Th/U colored according to the associated $^{207}Pb$-corrected $^{206}Pb/^{238}U$ date. Three broad fields of Hf concentration, <8,000 ppm, 8,000–10,150 ppm, and >10,150 ppm, are provided based on the short CART system of Belousova et al. (2002). The percentage of zircon within these fields that correspond to a specific rock type is provided for each field. The field for metamorphic zircon (i.e., Th/U < 0.1) is taken from Rubatto (2002). (b) Summary pie charts of inferred source rock type through time. Source rock type "other" refers to carbonatite, syenite, nepheline syenite, and monzonite (Belousova et al., 2002). This scheme has 80% probability of correctly classifying dolerite zircon, 64% probability of classifying basaltic zircon as sourced from basalt or dolerite, and 78 to 97% probability of correctly classifying granitoid zircon (Belousova et al., 2002). See Data Set S1 for full zircon trace element data set.

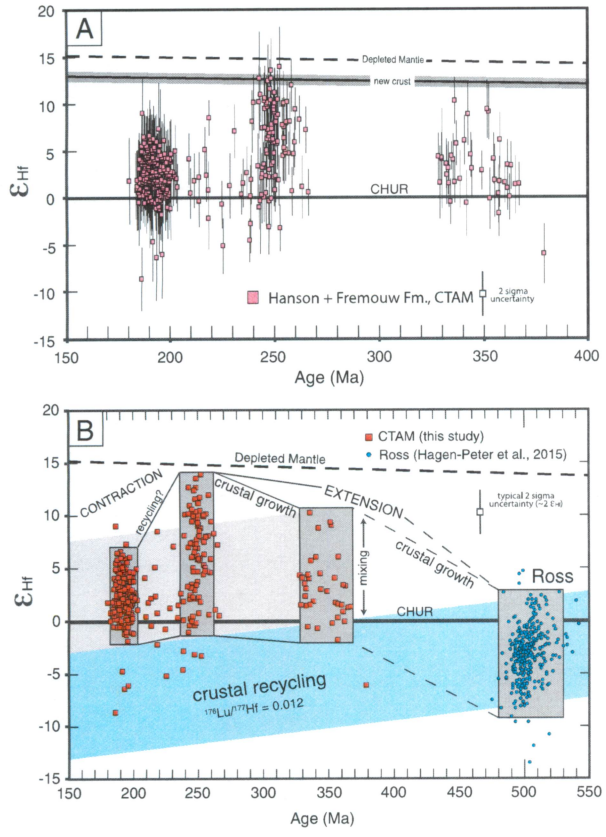


**Figure 6.** (a) Zircon age versus initial $\varepsilon_{Hf}$ plot summarizing all Hf isotopic data from this study. (b) Hf isotopic data from this study combined with data for the Ross Orogen from Hagen-Peter et al. (2015) and the inferred geodynamic evolution of the Antarctic sector arc system. Inclined gray and blue fields correspond to hypothetic fields of crustal recycling assuming a Lu/Hf = 0.012 (Rudnick & Gao, 2003). Hf isotopic values for depleted mantle and new crust are from Vervoort and Blichert-Toft (1999) and Dhuime et al. (2011). CHUR, chondritic uniform reservoir. See Data Set S2 for full zircon Hf isotope data set.

the zircon trace element data to define source rock type (Belousova et al., 2002). Figure 5 suggests a change in source rock type through time, from predominantly granitoid during the Ross Orogeny to dolerite in the Devonian-Jurassic arc, with 96% of zircon with >10,150 Hf ppm classified as granitoid, 97% with 8,000–10,150 Hf ppm classified as dolerite, and zircon with <8,000 Hf ppm classified as either basalt (89%) or carbonatite (11%) (Figure 5a). Overall, the average (±1 SD) zircon Hf concentration decreases through time from 10,850 ± 1,400 ppm during the Ross-Orogeny, 9,770 ± 1,560 ppm for the Devonian-Carboniferous, 9,630 ± 1,430 ppm for the Permian-Triassic, and 9,200 ± 1,420 ppm for the Early Jurassic. Similarly, the average (±1 SD) zircon Th/U increases steadily through time from 0.51 ± 0.29 during the Ross Orogeny to 1.06 ± 0.52 in the Early Jurassic and a small population of exclusively Ross age zircon yields zircon with Th/U < 0.1 potentially indicative of a metamorphic origin (Rubatto, 2002). Similarly, Figure 5b shows a decrease in granitoid source rock type from 62% during the Ross Orogeny to 21% in the Early Jurassic. This decrease is correlated with a concomitant increase in mafic source rock type (i.e., basalt + dolerite) from 31% during the Ross Orogeny to 77% in the Early Jurassic.

### 4.3. Hafnium Isotopes

Zircon Hf isotope data are provided in Data Set S2. To better characterize the geochemical evolution of post-Ross age arc magmatism, Lu-Hf isotopic measurements were exclusively made on 266–183 Ma and 367–328 Ma zircon subpopulations (Figure 6). These data are combined with recent data for the Ross Orogen (Hagen-Peter et al., 2015) to illustrate the zircon Hf isotopic evolution of the arc as recorded in the Transantarctic Mountains. Ninety-five percent of zircon with ages between 205 and 183 Ma ($n$ = 273) record initial $\varepsilon_{Hf}$ values of −1.8 to +6.6. Similarly, approximately 97% of zircon dated between 270 and 240 Ma ($n$ = 97) yield initial $\varepsilon_{Hf}$ values of −0.4 to +13.9, overlapping the "new crust" evolution line (Dhuime et al., 2011) and the depleted mantle evolution line (Vervoort & Blichert-Toft, 1999). Finally, all 367–328 Ma zircon ($n$ = 37) range from −1.8 to +10.3 initial $\varepsilon_{Hf}$.

## 5. Discussion

### 5.1. Zircon Geochronologic Record in the cTAM

The 266–183 Ma and 367–328 Ma subpopulations preserved in the Hanson and Fremouw formations provide a comprehensive archive of post-Ross age detrital zircon in the Beacon Supergroup consistent with, and significantly expanding on, the published data (Elliot & Fanning, 2008; Elliot et al., 2017; Elliot, Larsen, et al., 2016). Our data are characterized by large proportions of zircon ages close to the stratigraphic age of the sample (due to contemporaneous volcanism) and, therefore, reflect deposition adjacent to a magmatic arc along a convergent plate margin (Cawood et al., 2012). Consequently, our observations agree with those of Elliot, Fanning, et al. (2016), Elliot, Larsen, et al. (2016), and Elliot et al. (2017) who argue that these age ranges correspond to continuous periods of intensified volcanism in the arc directly outboard of the Transantarctic Basin. Previous workers have also thoroughly reviewed the provenance of the characteristic Gondwana signature observed in these rocks (Elliot et al., 2015; Elliot et al., 2017; Elliot, Larsen, et al., 2016).

Tuffs of the Hanson Formation are the best preserved sequence of volcaniclastic sediments in the TAM and contain fine to very fine grained silicic ash with distal Plinian eruption sources and medium-grained tuffs and accretionary lapilli that indicate more proximal sources (Elliot, Fanning, et al., 2016; Elliot, Larsen, et al., 2016). According to plate reconstructions, the arc would have been a maximum of 600–800 km from the cTAM in the Early Jurassic (Elliot, Fanning, et al., 2016; Elliot, Larsen, et al., 2016; Lawver et al., 2014). Although the

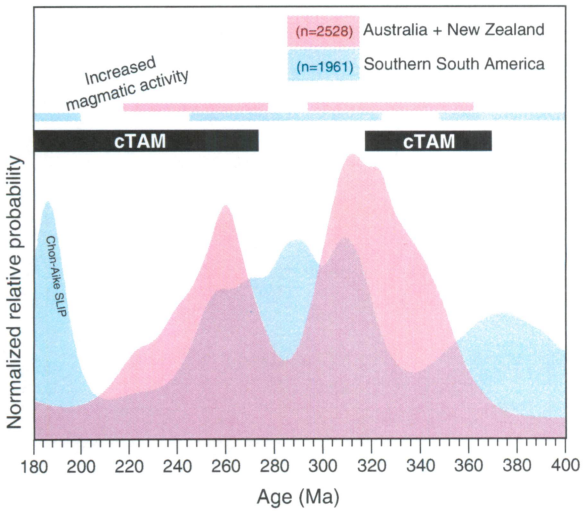


**Figure 7.** Compilation of detrital zircon data from Australia-Zealandia (red) and southern South America (blue). Increased magmatic activity corresponds to broad peaks in zircon growth. The range of zircon dates from the cTAM (this study) are provided in black for comparison. Data for Australia-Zealandia are from Adams, Korsch, and Griffin (2013), Scott et al. (2009, 2011), Li et al. (2015), Shaanan et al. (2015), and Murgulov et al. (2007). Data for southern South America are from new and compiled data of Pepper et al. (2016).

inferred ash transport distances are considerable, they are not without precedent. Recent workers have shown that Cretaceous supereruptions along the paleo-Pacific margin of Gondwana transported zircon some 2,300 km from their volcanic source (Barham et al., 2016). It is therefore reasonable to conclude that the detrital zircon record from the cTAM may be an integrated record of active volcanism from a significant portion of the outboard arc.

Existing detrital and crystalline basement zircon dates from West Antarctica, southern South America (i.e., Patagonia), Zealandia, and Australia indicate that all regions record overlapping periods of arc-related igneous activity in the Paleozoic and Mesozoic. A thorough review of the Devonian through Early Jurassic arc recorded in these regions is provided by Elliot (2013) and is therefore only briefly summarized here. In particular, granites and detrital zircon associated with the Lachlan and New England orogenies of Australia record a Devonian-Carboniferous and a Permian-Triassic arc (Adams, Korsch, & Griffin, 2013; Cawood, 2005; Cawood & Buchan, 2007; Cawood et al., 2011; Jeon et al., 2014; Kemp et al., 2009; Li et al., 2015; Phillips et al., 2011; Shaanan et al., 2015; Shaw et al., 2011; Veevers et al., 2006). The Median Batholith and volcaniclastic sediments of Zealandia contain a similar record of arc activity for these time periods (Adams et al., 2007; Adams, Korsch, Griffin, et al., 2013; Adams, Mortimer, et al., 2013; Allibone et al., 2009; Cawood et al., 1999; Kimbrough et al., 1994; Mortimer et al., 1999, 2014, 2015; Tulloch et al., 2009). Detrital and igneous dates for the southern section of the South American arc compiled by Pepper et al. (2016) provide a comprehensive record of near continuous activity with several pulses of increased magma production throughout the Paleozoic and Mesozoic. The record is more scattered in the ice-covered regions of West Antarctica (i.e., Marie Byrd Land, Thurston Island, the Ellsworth-Whitmore block, and the Antarctic Peninsula), but limited geochronologic data available suggest that the bedrock contains Devonian through Early Jurassic magmatic and volcanic rocks (Craddock, Fitzgerald, et al., 2017; Craddock, Schmitz, et al., 2017; Millar et al., 2002; Mukasa & Dalziel, 2000; Pankhurst et al., 1993; Riley et al., 2017; Yakymchuk et al., 2015).

Comparing the detrital zircon data from Pepper et al. (2016) to detrital zircon data from Australia and Zealandia (combined) illustrates broad differences in the timing of arc magmatic activity between these regions and the cTAM (Figure 7). The most important similarity between these regional data sets is that they both display a nearly continuous record of zircon dates from the Devonian through the Early Jurassic. However, an apparent difference emerges between the timing of pronounced peaks representing increased magmatic activity. Data from southern South America indicate increased magmatic activity from 400 to 350 Ma (or older) and 325 to 245 Ma and a sharp peak in the Early Jurassic that overlap with magmatic lulls (or gaps) in the data from Australia and Zealandia. Increased magmatic activity in Australia and Zealandia occurs from 360 to 295 Ma and 275 to 215 Ma, partially overlapping lulls in the South American data and the zircon peaks from the cTAM. Along-arc variation in episodic behavior similar to that observed here from South America to Zealandia-Australia has also been observed in other arcs and may indicate a major change in tectonism or subduction dynamics (Paterson & Ducea, 2015) between these two regions. The similarity between the cTAM zircon ages and the detrital zircon record from Australia and Zealandia suggests that they may have a shared history of tectonism and subduction and that a continuous arc system may have extended from Australia to Zealandia and outboard of the cTAM from the Devonian to at least the Triassic. Based on the difference in zircons etc., this arc system is likely to have been decoupled, at least temporally, from the southern South American sector arc.

Studies of the crystalline basement and detrital zircon record of the Antarctic Peninsula indicate that it is more closely related with the arc history of southern South America, that is, Patagonia, rather than Zealandia or Australia (Bradshaw et al., 2012; Castillo et al., 2015; Fanning et al., 2011). For this reason, and for comparative purposes, the Antarctic Peninsula data are grouped with the South American data.

### 5.2. Zircon Trace Element Petrochronology

As mentioned earlier, the rocks studied here contain older detrital zircon comprising a typical Gondwana signature (Figure 4). The presence of these zircon, as well as the range of zircon dates discussed above, in all of the samples included in this study, indicates that whole rock elemental and isotope geochemistry reflects the concentration-weighted cumulative contribution of material from numerous isotopically and temporally distinct reservoirs and therefore does not accurately record the time-resolved isotopic evolution of the magmatic source. For this reason we focus exclusively on zircon isotope and elemental geochemistry to track the geochemical evolution of the arc through time.

The zircon trace element data reported here is the first of its kind for Early Jurassic and Permian strata of the Transantarctic Mountains and provides insight into the geochemical evolution of the arc. The utility of detrital zircon trace element geochemistry is in relating the concentrations and ratios of key trace elements to a particular source rock type (Belousova et al., 2002), a tectonomagmatic setting (Grimes et al., 2015), and/or the concentration and/or ratio of various trace elements in the source rock (Chapman et al., 2016). These techniques have been met with some skepticism, partially due to the difficulty in determining reliable zircon/bulk rock trace element partition coefficients (Chapman et al., 2016; Hoskin & Ireland, 2000). Nevertheless, application of the techniques from Grimes et al. (2015) and Chapman et al. (2016) indicate that zircon from the cTAM fall on the magmatic arc array and have light rare earth element enrichment, typical of magmatic arcs (Figure S2), supporting our assertion that the source region(s) for the CTAM zircon is located in the arc outboard of the paleo-Pacific margin.

Application of the short "CART" classification tree of Belousova et al. (2002) yields apparent variations in rock type through time, with a mostly granitoid source rock during the Ross Orogeny and a predominantly mafic source rock (basalt and dolerite) for the Devonian-Jurassic arc (Figure 5). Zircon Hf concentration is a distinguishing characteristic of the short CART tree, and the data show a decrease in Hf concentration from the Ross Orogeny through the Devonian-Jurassic zircon ages indicating a switch to more juvenile mafic magmatism following the termination of the Ross Orogeny. The classification of dolerite or basalt for many of the Early Jurassic zircon from the Hanson Formation is apparently at odds with petrographic studies and whole rock geochemical data for Hanson tuffs that suggests a primarily rhyolitic source from explosive plinian eruptions interpreted to record silicic arc volcanism (Elliot, Fanning, et al., 2016; Elliot, Larsen, et al., 2016). In contrast, the designation of Ediacaran-Ordovician zircon as mostly granitoid appears to be an accurate classification as the corresponding Ross Orogen is dominated by granitic batholiths (e.g., Cox et al., 2000). The apparent mismatch between zircon geochemistry and bulk rock geochemistry of Permian-Early Jurassic volcaniclastic sediments may be a result of the relatively long transport distances. It has been demonstrated that during atmospheric transport, crystal fractionation can occur, modifying the apparent bulk composition of the resulting sediments (Fruchter et al., 1980; Hinkley et al., 1980; Taylor & Lichte, 1980). This suggests that the volcanic components in the Hanson and Fremouw formations may in fact reflect mafic volcanism rather than silicic. In any event, a decrease in zircon Hf concentration correlated with an increase in Th/U indicates that a more mafic, primitive, less evolved arc system (McKay et al., 2016) prevailed in Devonian through Early Jurassic time compared to the Ross Orogeny (Figure 5). This switch from felsic- to mafic-dominated magmatism may indicate the development of an extensional or retreating arc system following the termination of the advancing tectonics during the Ross Orogeny (Collins, 2002a).

### 5.3. Zircon Hafnium Isotopes and Geodynamic Evolution

The positive initial $\varepsilon_{Hf}$ values for Devonian and younger zircons contrast with negative values for zircon from granites of the Ross Orogen (Figure 6; Hagen-Peter et al., 2015; Hagen-Peter & Cottle, 2017). The relative change in zircon initial $\varepsilon_{Hf}$ through time in magmatic arcs has been linked to the tectonic evolution of the arc (Kemp et al., 2009). In particular, Kemp et al. (2009) argued that a relative increase in initial $\varepsilon_{Hf}$ is indicative of a retreating arc system associated with an outboard migration of subduction zone magmatism during slab rollback and associated crustal extension and thinning. The increase in initial $\varepsilon_{Hf}$ in the inferred retreating arc system results from a reduced amount of crustal assimilation during crustal extension and thinning and/or melting of upwelling-depleted asthenospheric mantle. Conversely, an advancing arc system is associated with a decrease in the initial $\varepsilon_{Hf}$ composition during periods of compression when the slab is advancing and the arc is contracting (i.e., crustal thickening). Hf compositions decrease in advancing arc systems due to increasing crustal assimilation during crustal thickening and/or mantle enrichment by an elevated

contribution of subducted material to the mantle wedge. This model of "tectonic switching" (Collins, 2002a) provides a conceptual framework within which to interpret the data from the cTAM. It should be noted, however, that alternatives to the Collins (2002a) model used here have been proposed for the paleo-Pacific margin of Gondwana (Aitchison & Buckman, 2012; Crawford, 2003; Gibson et al., 2015). These models generally support "quantum tectonics" which refers to switching of subduction polarity, subduction flip, along the Gondwana margin resulting in periods of island arc formation, accretion, and switch to continental arc formation (Aitchison & Buckman, 2012). This is in contrast to the "accordion tectonics" hypothesis endorsed in this study that supports a nearly continuous continental arc, that is, accretionary orogen undergoing periods of extension during slab retreat and compression during slab advance (Cawood et al., 2009; Collins, 2002a). For our purposes, we interpret our data within the model of accretionary orogenesis because it has been widely applied to zircon Hf isotope data sets along the paleo-Pacific margin of Gondwana (e.g., Kemp et al., 2009; Li et al., 2015; Pepper et al., 2016; Phillips et al., 2011; Rey et al., 2016), and there remains no consensus on the appropriate tectonic model for the evolution of the margin (Aitchison & Buckman, 2013; Fergusson, 2013).

Recent studies suggest that the Ross Orogeny mantle source was significantly modified due to the addition of subducted ancient crustal material, producing a mantle source with enriched, unradiogenic initial $\varepsilon_{Hf}$ compositions (Couzinié et al., 2016; Hagen-Peter et al., 2015). Consequently, the positive initial $\varepsilon_{Hf}$ values for zircon younger than the Ordovician cannot be explained without the addition of a juvenile, primitive depleted mantle component to the arc magma source region(s) following the Ross Orogeny. For this reason the increase in initial $\varepsilon_{Hf}$ from the Ordovician to the Devonian is interpreted as a change in the tectonic conditions from an advancing arc system undergoing crustal thickening and crustal recycling in the Ross Orogeny to a retreating arc system undergoing extension and reduced crustal recycling in the Devonian-Carboniferous (Cawood & Buchan, 2007). The period between the Ordovician and Devonian that contains few zircon ages possibly represents a magmatic lull in the Antarctic sector arc, but the lack of data precludes us from determining the precise time of tectonic switching from an advancing to a retreating system. Even though Devonian-Carboniferous magmas represent increased juvenile mantle melting compared to the Ross Orogeny, the zircon initial $\varepsilon_{Hf}$ is still far below the depleted mantle evolution line and also varies considerably from $-2$ to $+10$. The variation in Hf composition is interpreted to represent a minor contribution of subducted crustal material in an already heterogeneous mantle source and/or variable crustal assimilation during magma ascent. In either case, only a few of the lowest initial $\varepsilon_{Hf}$ zircon from the Devonian-Carboniferous can be explained by complete recycling of Ross-aged or older crust (assuming a Lu/Hf = 0.012; Rudnick & Gao, 2003). A similar case can be made for Permian-Triassic zircon, in which the $\varepsilon_{Hf}$ ranges from 0 to +14 with an overall increase in the initial $\varepsilon_{Hf}$ composition through time. This suggests generation of juvenile crust related to continued extension and outboard migration of the magmatic arc during slab retreat in the Late Permian to Early Triassic. The large variation in initial $\varepsilon_{Hf}$ is again interpreted as reflecting a heterogeneous mantle source and/or assimilation of crust during ascent. Much of the Permian-Triassic initial $\varepsilon_{Hf}$ data, however, can be explained by recycling of juvenile Devonian-Carboniferous crust (assuming a Lu/Hf = 0.012), so the degree of crustal growth in the Permian-Triassic is inferred to be limited. It is probable that Permian-Triassic magmas ascended through juvenile crust produced in the Devonian-Carboniferous as well as older crust (i.e., Ross, Grenville, etc.) and assimilated multiple crustal reservoirs. This makes it difficult to assess the amount of crustal growth that may have occurred during this time period.

In the Early Jurassic, initial $\varepsilon_{Hf}$ zircon composition shifts to more intermediate values of $-1.8$ to +6.6, indicating increased crustal recycling relative to the Triassic. It is unclear whether these lower initial $\varepsilon_{Hf}$ compositions are generated by subduction modification of the mantle source and/or by crustal assimilation; however, a relative decrease in initial $\varepsilon_{Hf}$ implies a contraction of the magmatic arc during a switch to an advancing tectonic regime. The full range of initial $\varepsilon_{Hf}$ for the Early Jurassic can be explained by recycling of Devonian-Carboniferous and Permo-Triassic crust (assuming a Lu/Hf = 0.012, Figure 6).

### 5.4. Pan-Paleo-Pacific Margin Hf Isotopes

Our new zircon Hf isotope data enable the first opportunity to make broad comparisons between the cTAM and other portions of the paleo-Pacific margin of Gondwana. In Figure 8a we provide compilations of both zircon and whole-rock Hf isotope data from igneous rocks and detrital zircon separated into two regions, Australia and Zealandia (red), and South America (blue), and fields of major groupings of data from

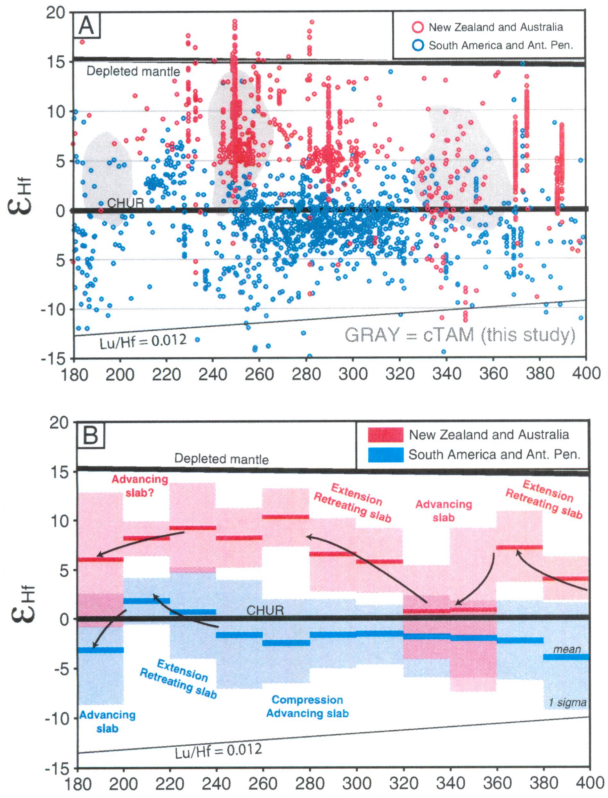


**Figure 8.** (a) Compilation of zircon Hf isotope data from Australia-Zealandia (red) and South America-Antarctic Peninsula (blue). Fields for Hf isotope data from the cTAM (this study) are provided in gray. Data for Australia-Zealandia are from Veevers et al. (2006), Li et al. (2015), Shaw et al. (2011), Phillips et al. (2011), Kemp et al. (2009, 2007, 2005), Jeon et al. (2014), Regmi et al. (2016), Murgulov et al. (2007), Nebel et al. (2007), Hiess et al. (2015), Scott et al. (2009), and Milan et al. (2016). Data from South America-Antarctica Peninsula are from Bahlburg et al. (2009), Flowerdew et al. (2006), Bradshaw et al. (2012), Castillo et al. (2015), Fanning et al. (2011), Pepper et al. (2016), Rey et al. (2016), Pankhurst et al. (2016), and Canile et al., 2016. (b) Mean and 1 sigma uncertainty for data from Figure 8a grouped into 20 Myr bins, and the inferred intervals of increasing or decreasing initial $\varepsilon_{Hf}$ combined with geodynamic interpretations. Hf isotopic values for depleted mantle and new crust are from Vervoort and Blichert-Toft (1999). CHUR, chondritic uniform reservoir.

the cTAM (gray). These comparisons allow tracking of correlations inferred for arc systems and subduction dynamics through time to determine periods in which the Antarctic sector arc may have been coupled tectonically and geochemically with the Australian arc system, the South American arc system, or neither (decoupled). Devonian-Carboniferous zircon Hf data from the cTAM is generally positive and overlaps with data from Australia, Zealandia, and South America. Only data from Australia and Zealandia, however, overlap with the most positive values from the cTAM during this time. Permo-Triassic zircons from the cTAM, on the other hand, are highly positive and overlap almost entirely with data from Zealandia and Australia and only partially with low initial $\varepsilon_{Hf}$ values from South America.

The overlap of Permo-Triassic initial $\varepsilon_{Hf}$ between Australia-Zealandia and the cTAM zircon is a salient observation because it indicates a major period of crustal growth, extension, and slab retreat that was continuous along the arc from Australia through Zealandia, to outboard of the cTAM (Figures 8 and 9). This is consistent with a stepping out in the position of the plate boundary along Australia and Antarctica during the late Paleozoic to Mesozoic Gondwanide Orogen (Cawood, 2005). The Early Jurassic zircon Hf record from Australia and Zealandia is limited, with only six individual zircon measurements available. Nevertheless, the data from the cTAM overlap with data from both Australia and Zealandia and South America. South American zircon Hf values have a considerable range with a significant number of negative initial $\varepsilon_{Hf}$ values that indicate a difference between the South American Early Jurassic arc and the arc outboard of the cTAM. Overall, the generally positive initial $\varepsilon_{Hf}$ compositions from the Ordovician through the Early Jurassic correlate strongly with the positive initial $\varepsilon_{Hf}$ compositions of the Zealandia and Australian sectors of the margin but contrast strongly with the negative values recorded in the South American sector.

To support this postulated shared history between Antarctic and Australian sectors, mean initial $\varepsilon_{Hf}$ values are calculated in 20 Myr bins for Zealandia and Australia (red), and South America (blue) (Figure 8b). Calculating mean values enables a more statistically rigorous determination of periods of increasing or decreasing Hf isotope compositions through time and allows identification of periods in which the Australian and South American arc system are geochemically and tectonically decoupled. The Paleozoic history of the Australian arc system, as inferred from this compilation, includes extension, crustal growth, and slab retreat during the Devonian, a period of slab advance and increased recycling in the Carboniferous, and a shift back to crustal growth during slab retreat and extensional tectonics that persists until at least the Middle Triassic. These inferred tectonic switches based on our compilation of Hf isotope data are consistent with, and reinforce, the findings of Kemp et al. (2009). The Late Triassic and Early Jurassic data from Australia and Zealandia are limited but may indicate a switch to slab advance. Overall, the mean Hf isotopic evolution of the Australian sector arc system represents an extensional (retreating) arc system or orogen (Cawood et al., 2009; Collins, 2002b; Kemp et al., 2009) with major periods of crustal growth during extension and outboard migration of the arc associated with slab rollback.

In contrast to the Australia and Zealandia segment, the Hf compilation from the South American sector illustrates a significantly different inferred geodynamic evolution. In particular, the Paleozoic history is dominated by relatively constant, negative initial $\varepsilon_{Hf}$ compositions, indicating increased recycling of ancient crust during slab advance, consistent with previous work (Bahlburg et al., 2009; Pepper et al., 2016). The Late Triassic history of South America reported by Hervé et al. (2014) includes a shift to positive $\varepsilon_{Hf}$ values and extension

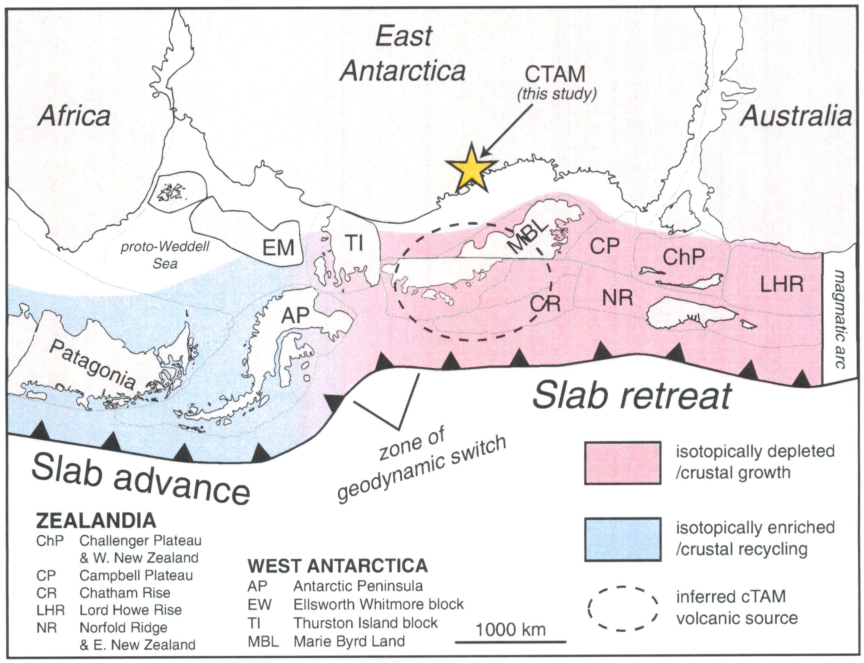


**Figure 9.** Reconstruction of the Gondwana plate margin, approximately Permian (Elliot, 2013). Shown are the inferred limits of the continuous retreating arc system that is isotopically depleted (red) and the advancing arc system that is isotopically enriched (blue). The zone of the geochemical and geodynamic switch occurs in the vicinity of the Thurston Island block. The region outboard of the cTAM is interpreted to be the isotopically depleted arc source for volcaniclastic sediments of the cTAM.

following the Gondwanide Orogeny. During Early Jurassic time initial $\varepsilon_{Hf}$ values return to negative values, suggesting a switch back to advancing tectonics and crustal recycling.

Overall, the initial $\varepsilon_{Hf}$ composition of the South American arc remains fairly negative throughout the Paleozoic and Early Mesozoic, suggesting that the subduction zone remained proximal to the continental margin and recycling ancient crust in an advancing arc system (Cawood et al., 2009). Previous authors have noted this along-arc geochemical and geodynamic variation between South America and Australia (Collins et al., 2011), but the nature of the arc between these two regions (i.e., Antarctica) has, until now, remained largely unknown. Castillo et al. (2015) observed a general increase in Permian detrital zircon initial $\varepsilon_{Hf}$ from Patagonia to the Antarctic Peninsula and attributed it to decreased sediment erosion and subduction due to Mesozoic glaciation. Similarly, in our compilation we observe an increase in initial $\varepsilon_{Hf}$ during periods of glaciation in eastern Australia from the mid-Carboniferous (circa 327 Ma) to the early Late Permian (circa 260 Ma) (Figure 8b; Fielding et al., 2008) that may also correspond to reduced sediment erosion and subsequent subduction rather than a switch to a retreating arc system, as is suggested here. This process, however, cannot explain the high initial $\varepsilon_{Hf}$ during the Late Permian–Early Triassic (circa 250 Ma) in nonglaciated eastern Australia that match well with our data from the cTAM. We would expect a significant decrease in the initial $\varepsilon_{Hf}$ during nonglacial periods (e.g., circa 250 Ma) if arc chemistry were controlled by fluctuations in continental erosion related to glaciation rather than geodynamics of the arc system. Instead, it is argued that major periods of juvenile crustal growth during slab retreat and outboard migration of the Antarctic sector arc reflect the continuity of the Australian sector retreating arc into the regions outboard of the TAM, namely Marie Byrd Land and crustal blocks of Zealandia (Figure 9). This connection is further supported by similarities in zircon ages from the cTAM and detrital zircon from Australia and Zealandia, as discussed above (Figure 7), and a switch to mafic volcanism indicative of retreating arc systems as identified in our zircon trace element data (Collins, 2002b).

Permian plate reconstructions combined with these new observations indicate that the locus of a major along-arc geochemical and geodynamic shift between Australia and South America occurred in the vicinity of the Thurston Island block and the surrounding area in West Antarctica (Figure 9). These regions have limited combined precise geochronologic and isotopic data, for example, zircon U-Pb and Hf isotopes, for

Late Paleozoic and Mesozoic rocks. In Marie Byrd Land, the Ford granodiorite suite (375–345) has initial $\varepsilon_{Hf}$ values ranging from +2 to −5 (Yakymchuk et al., 2015). On Thurston Island, a granodioritic gneiss (349 Ma) has an initial $\varepsilon_{Hf}$ ranging from +10 to +2, and a Middle Triassic diorite (239 Ma) has an initial $\varepsilon_{Hf}$ ranging from +0.3 to −7.6 (Riley et al., 2017). Despite the limited data set, diorite from Thurston Island has similar initial $\varepsilon_{Hf}$ values to those from the Antarctic Peninsula (Flowerdew et al., 2006) and may reflect a continuity of the South American sector Permo-Triassic advancing arc system. Currently, there are no Permian-Jurassic zircon Hf data available from Marie Byrd Land. However, a granite at Kinsey Ridge in Marie Byrd Land has a Rb-Sr isochron age of 239 ± 4 Ma and an initial $\varepsilon_{Nd}$ value of +4.7 that corresponds to an initial $\varepsilon_{Hf}$ value of +9.2, (using the Nd-Hf conversion equation from Vervoort & Blichert-Toft (1999). This hints at a possible source for Middle Triassic zircon in the cTAM and that a record of Permo-Triassic crustal growth may be present in the Admundsen province of Marie Byrd Land. Ultimately, limited available data support a possible Marie Byrd Land source for the zircon in the cTAM and validate reconstructions that place proto-Marie Byrd Land directly outboard of the TAM in the Paleozoic.

## 6. Conclusions

Zircon from volcaniclastic sediments in the cTAM record the timing and geochemical evolution of the Paleozoic-Mesozoic magmatic arc along the paleo-Pacific margin of Gondwana. Post-Ross age zircon corresponds to periods of arc volcanism at 266–183 Ma and 367–328 Ma. Zircon trace element geochemistry is consistent with a more mafic source rock type (i.e., basalt and dolerite) than previously reported and a continental magmatic arc setting. The generally positive initial $\varepsilon_{Hf}$ zircon values represent juvenile crustal growth during a major period of long-lived slab rollback and upper plate extension that began shortly after, or synchronous with, the termination of the Ross Orogeny. The Hf isotope data record a geodynamic history for the Antarctic sector of the arc that is similar to the Australian sector arc and indicates continuity of an extensional arc system from Australia to Antarctica after ~500 Ma. This extensional arc system underwent an along-arc tectonic switch to advancing compressional tectonism in the South American sector arc throughout at least the Permian.

**Acknowledgments**

This material is based upon work supported by the National Science Foundation Graduate Research Fellowship under grant 1650114 and support from NSF-ANT-1443296 and NSF-ANT-1043152. We are grateful to Anne Grunow and the Polar Rock Repository for providing samples and assisting with sample selection. We also acknowledge the original sample collectors: P. J. Barrett and D. H. Elliot. Special thanks go to S. Briggs and R. Holder for fruitful discussions and constructive criticism during preparation of this manuscript. Constructive reviews by P. Cawood, G. Gibson, and the Associate Editor, J. Aitcheson, significantly improved this manuscript. Additional analytical details and data tables can be obtained in the supporting information and data sets.

## References

Adams, C. J., Barley, M. E., Maas, R., & Doyle, M. G. (2002). Provenance of Permian-Triassic volcaniclastic sedimentary terranes in New Zealand: Evidence from their radiogenic isotope characteristics and detrital mineral age patterns. *New Zealand Journal of Geology and Geophysics*, *45*(2), 221–242. https://doi.org/10.1080/00288306.2002.9514970

Adams, C. J., Campbell, H. J., & Griffin, W. L. (2007). Provenance comparisons of Permian to Jurassic tectonostratigraphic terranes in New Zealand: Perspectives from detrital zircon age patterns. *Geological Magazine*, *144*(04), 701–729. https://doi.org/10.1017/S0016756807003469

Adams, C. J., Korsch, R. J., & Griffin, W. L. (2013). Provenance comparisons between the Nambucca Block, eastern Australia and the Torlesse composite terrane, New Zealand: Connections and implications from detrital zircon age patterns. *Australian Journal of Earth Sciences*, *60*(2), 241–253. https://doi.org/10.1080/08120099.2013.767282

Adams, C. J., Korsch, R. J., Griffin, W. L., Division, N. H., Box, G. P. O., Sciences, P., … Road, A. S. (2013). Provenance comparisons between the Nambucca Block, eastern Australia and the Torlesse composite terrane, New Zealand : Connections and implications from detrital zircon age patterns GNS science, Private Bag 1930, Dunedin 9054, New Zealand. GEMOC and:

Adams, C. J., Mortimer, N., Campbell, H. J., & Griffin, W. L. (2013). Detrital zircon geochronology and sandstone provenance of basement Waipapa terrane (Triassic–Cretaceous) and Cretaceous cover rocks (Northland Allochthon and Houhora complex) in northern North Island New Zealand. *Geological Magazine*, *150*(01), 89–109. https://doi.org/10.1017/s0016756812000258

Aitchison, J. C., & Buckman, S. (2012). Accordion vs. quantum tectonics: Insights into continental growth processes from the Paleozoic of eastern Gondwana. *Gondwana Research*, *22*(2), 674–680. https://doi.org/10.1016/j.gr.2012.05.013

Aitchison, J. C., & Buckman, S. (2013). Reply to comment on "Accordion vs. quantum tectonics: Insights into continental growth processes from the Paleozoic of eastern Gondwana". *Gondwana Research*, *22*(2), 674–680. https://doi.org/10.1016/j.gr.2012.05.013

Allibone, A. H., Jongens, R., Scott, J. M., Tulloch, A. J., Turnbull, I. M., Cooper, A. F., … Rattenbury, M. S. (2009). Plutonic rocks of the Median Batholith in eastern and central Fiordland, New Zealand: Field relations, geochemistry, correlation, and nomenclature. *New Zealand Journal of Geology and Geophysics*, *52*(2), 101–148. https://doi.org/10.1080/00288300909509882

Andersen, T. (2002). Correction of common lead in U–Pb analyses that do not report $^{204}$Pb. *Chemical Geology*, *192*(1-2), 59–79. https://doi.org/10.1016/S0009-2541(02)00195-X

Bahlburg, H., Vervoort, J. D., Du Frane, S. A., Bock, B., Augustsson, C., & Reimann, C. (2009). Timing of crust formation and recycling in accretionary orogens: Insights learned from the western margin of South America. *Earth-Science Reviews*, *97*(1-4), 215–241. https://doi.org/10.1016/j.earscirev.2009.10.006

Barham, M., Kirkland, C. L., Reynolds, S., O'Leary, M. J., Evans, N. J., Allen, H., … Goodall, J. (2016). The answers are blowin' in the wind: Ultra-distal ashfall zircons, indicators of Cretaceous super-eruptions in eastern Gondwana. *Geology*, *44*(8), 643–646. https://doi.org/10.1130/G38000.1

Barrett, P. J., Elliot, D. H., & Lindsay, J. F. (1986). The Beacon Supergroup (Devonian-Triassic) and Ferrar Group (Jurassic) in the Beardmore Glacier area, Antarctica. In M. D. Turner & J. E. Splettstoesser (Eds.), *Geology of the central Transantarctic Mountains*, *Antarctic Research Series* (Vol. 36, pp. 339–428). Washington, DC: American Geophysical Union. https://doi.org/10.1029/AR036p0339

Belousova, E., Griffin, W., O'Reilly, S. Y., & Fisher, N. (2002). Igneous zircon: Trace element composition as an indicator of source rock type. *Contributions to Mineralogy and Petrology*, *143*(5), 602–622. https://doi.org/10.1007/s00410-002-0364-7

Blichert-Toft, J. (2008). The Hf isotopic composition of zircon reference material 91500. *Chemical Geology*, *253*(3-4), 252–257. https://doi.org/10.1016/j.chemgeo.2008.05.014

Bradshaw, J. D., Vaughan, A. P. M., Millar, I. L., Flowerdew, M. J., Trouw, R. A. J., Fanning, C. M., & Whitehouse, M. J. (2012). Permo-Carboniferous conglomerates in the trinity peninsula Group at View Point, Antarctic Peninsula : Sedimentology, geochronology and isotope evidence for provenance and tectonic setting in Gondwana. *Geological Magazine*, *149*(04), 626–644. https://doi.org/10.1017/S001675681100080X

Burgess, S. D., Bowring, S. A., Fleming, T. H., & Elliot, D. H. (2015). High-precision geochronology links the Ferrar Large Igneous Province with early-Jurassic ocean anoxia and biotic crisis. *Earth and Planetary Science Letters*, *415*, 90–99. https://doi.org/10.1016/j.epsl.2015.01.037

Canile, F. M., Babinski, M., & Rocha-Campos, A. C. (2016). Evolution of the Carboniferous-Early Cretaceous units of Paraná Basin from provenance studies based on U-Pb, Hf and O isotopes from detrital zircons. *Gondwana Research*, *40*, 142–169. https://doi.org/10.1016/j.gr.2016.08.008

Castillo, P., Fanning, C. M., Hervé, F., & Lacassie, J. P. (2015). Characterisation and tracing of Permian magmatism in the south-western segment of the Gondwanan margin; U-Pb age, Lu-Hf and O isotopic compositions of detrital zircons from metasedimentary complexes of northern Antarctic Peninsula and western Patagonia. *Gondwana Research*, *36*, 1–13. https://doi.org/10.1016/j.gr.2015.07.014

Cawood, P. A. (2005). Terra Australis Orogen: Rodinia breakup and development of the Pacific and Iapetus margins of Gondwana during the Neoproterozoic and Paleozoic. *Earth-Science Reviews*, *69*(3-4), 249–279. https://doi.org/10.1016/j.earscirev.2004.09.001

Cawood, P. A., & Buchan, C. (2007). Linking accretionary orogenesis with supercontinent assembly. *Earth-Science Reviews*, *82*(3-4), 217–256. https://doi.org/10.1016/j.earscirev.2007.03.003

Cawood, P. A., Hawkesworth, C. J., & Dhuime, B. (2012). Detrital zircon record and tectonic setting. *Geology*, *40*(10), 875–878. https://doi.org/10.1130/G32945.1

Cawood, P. A., Kröner, A., Collins, W. J., Kusky, T. M., Mooney, W. D., & Windley, B. F. (2009). Accretionary orogens through Earth history. *Geological Society, London, Special Publications*, *318*(1), 1–36. https://doi.org/10.1144/SP318.1

Cawood, P. A., Leitch, E. C., Merle, R. E., & Nemchin, A. A. (2011). Orogenesis without collision: Stabilizing the Terra Australis accretionary orogen, eastern Australia. *Bulletin of the Geological Society of America*, *123*(11-12), 2240–2255. https://doi.org/10.1130/B30415.1

Cawood, P. A., Nemchin, A. A., Leverenz, A., Saeed, A., & Ballance, P. F. (1999). U/Pb dating of detrital zircons: Implications for the provenance record of Gondwana margin terranes. *Bulletin of the Geological Society of America*, *111*(8), 1107–1119. https://doi.org/10.1130/0016-7606(1999)111%3C1107:UPDODZ%3E2.3.CO;2

Chapman, J. B., Gehrels, G. E., Ducea, M. N., Giesler, N., & Pullen, A. (2016). A new method for estimating parent rock trace element concentrations from zircon. *Chemical Geology*, *439*, 59–70. https://doi.org/10.1016/j.chemgeo.2016.06.014

Chu, N.-C., Taylor, R. N., Chavagnac, V., Nesbitt, R. W., Boella, R. M., Milton, J. A., … Burton, K. (2002). Hf isotope ratio analysis using multi-collector inductively coupled plasma mass spectrometry: An evaluation of isobaric interference corrections. *Journal of Analytical Atomic Spectrometry*, *17*(12), 1567–1574. https://doi.org/10.1039/b206707b

Collins, W. J. (2002a). Hot orogens, tectonic switching, and creation of continental crust. *Geology*, *30*(6), 535–538. https://doi.org/10.1130/0091-7613(2002)030%3C0535:HOTSAC%3E2.0.CO;2

Collins, W. J. (2002b). Nature of extensional accretionary orogens. *Tectonics*, *21*4, 1024. https://doi.org/10.1029/2000TC001272

Collins, W. J., Belousova, E. A., Kemp, A. I. S., & Murphy, J. B. (2011). Two contrasting Phanerozoic orogenic systems revealed by hafnium isotope data. *Nature Geoscience*, *4*(5), 333–337. https://doi.org/10.1038/ngeo1127

Collinson, J. W., & Elliot, D. H. (1984). Triassic stratigraphy of the Shackleton Glacier area. In M. D. Turner & J. E. Splettstoesser (Eds.), *Geology of the central Transantarctic Mountains* (pp. 103–117). Washington, DC: American Geophysical Union. https://doi.org/10.1029/AR036p0103

Collinson, J. W., Isbell, J. L., Elliot, D. H., Miller, M. F., Miller, J. M. G., & Veevers, J. J. (1994). Permian-Triassic Transantarctic basin. In J. J. Veevers & C. M. A. Powell (Eds.), *Permian–Triassic Pangean basins and foldbelts along the Panthalassan margin of Gondwanaland*, *Geological society of America Memoirs* (Vol. 184, pp. 173–222). https://doi.org/10.1130/MEM184-p173

Couzinié, S., Laurent, O., Moyen, J.-F., Zeh, A., Bouilhol, P., & Villaros, A. (2016). Post-collisional magmatism: Crustal growth not identified by zircon Hf–O isotopes. *Earth and Planetary Science Letters*, *456*, 182–195. https://doi.org/10.1016/j.epsl.2016.09.033

Cox, S. C., Parkinson, D. L., Allibone, A. H., & Cooper, A. F. (2000). Isotopic character of Cambro-Ordovician plutonism, southern Victoria Land, Antarctica. *New Zealand Journal of Geology and Geophysics*, *43*(4), 501–520. https://doi.org/10.1080/00288306.2000.9514906

Craddock, J. P., Fitzgerald, P., Konstantinou, A., Nereson, A., & Thomas, R. J. (2017). Detrital zircon provenance of Upper Cambrian-Permian strata and tectonic evolution of the Ellsworth Mountains, West Antarctica. *Gondwana Research*, *45*, 191–207. https://doi.org/10.1016/j.gr.2016.11.011

Craddock, J. P., Schmitz, M. D., Crowley, J. L., Larocque, J., Pankhurst, R. J., Juda, N., … Storey, B. (2017). Precise U-Pb zircon ages and geochemistry of Jurassic granites, Ellsworth-Whitmore terrane, central Antarctica. *Geological Society of America Bulletin*, *129*(1-2), 118–136. https://doi.org/10.1130/B31485.1

Crawford, A. (2003). 120 to 0 Ma tectonic evolution of the southwest Pacific and analogous geological evolution of the 600 to 220 Ma Tasman Fold Belt system. *Geological Society of Australia Special Publication*, *372*, 377–397. https://doi.org/10.1130/0-8137-2372-8.383

Dalziel, I. W. D., & Elliot, D. H. (1982). West Antarctica: Problem child of Gondwanaland. *Tectonics*, *1*(1), 3–19. https://doi.org/10.1029/TC001i001p00003

Dhuime, B., Hawkesworth, C., & Cawood, P. (2011). When continents formed. *Science*, *331*(6014), 154–155. https://doi.org/10.1126/science.1201245

Elliot, D. H. (1996). The Hanson formation: A new stratigraphical unit in the Transantartic Mountains, Antarctica. *Antarctic Science*, *8*(04). https://doi.org/10.1017/S0954102096000569

Elliot, D. H. (2000). Stratigraphy of Jurassic pyroclastic rocks in the Transantarctic Mountains. *Journal of African Earth Sciences*, *31*(1), 77–89. https://doi.org/10.1016/S0899-5362(00)00074-9

Elliot, D. H. (2013). The geological and tectonic evolution of the Transantarctic Mountains: A review. *Geological Society, London, Special Publications*, *381*(1), 7–35. https://doi.org/10.1144/SP381.14

Elliot, D. H., & Fanning, C. M. (2008). Detrital zircons from upper Permian and lower Triassic Victoria Group sandstones, Shackleton Glacier region, Antarctica: Evidence for multiple sources along the Gondwana plate margin. *Gondwana Research*, *13*(2), 259–274. https://doi.org/10.1016/j.gr.2007.05.003

Elliot, D. H., Fleming, T. H., Foland, K. A., & Fanning, C. M. (2007). Jurassic silicic volcanism in the Transantarctic Mountains: Was it related to plate margin processes or to Ferrar magmatism. In A. K. Cooper, et al. (Eds.), *Antarctica: A Keystone in a Changing World - Online Proceedings of the 10th ISAES, USGS Open-File Report 2007-1047, Short Research Paper 051* (5 p.). https://doi.org/10.3133/of2007-1047.srp051

Elliot, D. H., Fanning, C. M., & Hulett, S. R. W. (2015). Age provinces in the Antarctic craton: Evidence from detrital zircons in Permian strata from the Beardmore Glacier region, Antarctica. *Gondwana Research*, *28*(1), 152–164. https://doi.org/10.1016/j.gr.2014.03.013

Elliot, D. H., Fanning, C. M., Isbell, J. L., & Hulett, S. R. W. (2017). The Permo-Triassic Gondwana sequence, central Transantarctic Mountains, Antarctica: Zircon geochronology, provenance, and basin evolution. *Geosphere*, *13*(1), 155–178. https://doi.org/10.1130/GES01345.1

Elliot, D. H., Fanning, C. M., & Laudon, T. S. (2016). The Gondwana plate margin in the Weddell Sea sector: Zircon geochronology of upper Paleozoic (mainly Permian) strata from the Ellsworth Mountains and eastern Ellsworth Land, Antarctica. *Gondwana Research*, *29*(1), 234–247. https://doi.org/10.1016/j.gr.2014.12.001

Elliot, D. H., & Fleming, T. H. (2004). Occurrence and dispersal of magmas in the Jurassic Ferrar Large Igneous Province, Antarctica. *Gondwana Research*, *7*(1), 223–237. https://doi.org/10.1016/S1342-937X(05)70322-1

Elliot, D. H., Larsen, D., Fanning, C. M., Fleming, T. H., & Vervoort, J. D. (2016). The Lower Jurassic Hanson formation of the Transantarctic Mountains: Implications for the Antarctic sector of the Gondwana plate margin. *Geological Magazine*, *154*(04), 777–803. https://doi.org/10.1017/S0016756816000388

Elsner, M., Schöner, R., Gerdes, A., & Gaupp, R. (2013). Reconstruction of the early Mesozoic plate margin of Gondwana by U–Pb ages of detrital zircons from northern Victoria Land, Antarctica. *Geological Society, London, Special Publications*, *383*(1), 211–232. https://doi.org/10.1144/SP383.5

Fanning, C. M., Hervé, F., Pankhurst, R. J., Rapela, C. W., Kleiman, L. E., Yaxley, G. M., & Castillo, P. (2011). Lu–Hf isotope evidence for the provenance of Permian detritus in accretionary complexes of western Patagonia and the northern Antarctic Peninsula region. *Journal of South American Earth Sciences*, *32*(4), 485–496. https://doi.org/10.1016/j.jsames.2011.03.007

Fergusson, C. L. (2013). Comment on "Accordion vs. quantum tectonics: Insights into continental growth processes from the Paleozoic of eastern Gondwana" by Jonathan C. Aitchison, Solomon Buckman Gondwana Research, volume 22, issue 2, September 2012, pages 674–680. *Gondwana Research*, *23*(4), 1646–1649. https://doi.org/10.1016/j.gr.2012.12.013

Fielding, C. R., Frank, T. D., Birgenheier, L. P., Rygel, M. C., Jones, A. T., & Roberts, J. (2008). Stratigraphic imprint of the late Palaeozoic ice age in eastern Australia: A record of alternating glacial and nonglacial climate regime. *Journal of the Geological Society*, *165*(1), 129–140. https://doi.org/10.1144/0016-76492007-036

Flowerdew, M. J., Millar, I. L., Vaughan, A. P. M., Horstwood, M. S. A., & Fanning, C. M. (2006). The source of granitic gneisses and migmatites in the Antarctic Peninsula: A combined U–Pb SHRIMP and laser ablation Hf isotope study of complex zircons. *Contributions to Mineralogy and Petrology*, *151*(6), 751–768. https://doi.org/10.1007/s00410-006-0091-6

Foden, J., Elburg, M. A., Dougherty-Page, J., & Burtt, A. (2006). The timing and duration of the Delamerian orogeny: Correlation with the Ross Orogen and implications for Gondwana assembly. *The Journal of Geology*, *114*(2), 189–210. https://doi.org/10.1086/499570

Fruchter, J. S., Robertson, D. E., Evans, J. C., Olsen, K. B., Lepel, E. A., Laul, J. C., … Cannon, W. C. (1980). Mount St. Helens Ash from the 18 May 1980, Eruption: Chemical, physical, mineralogical, and biological properties. *Science*, *209*(4461), 1116–1125. https://doi.org/10.1126/science.209.4461.1116

Gibson, G. M., Champion, D. C., & Ireland, T. R. (2015). Preservation of a fragmented late Neoproterozoic-earliest Cambrian hyper-extended continental-margin sequence in the Australian Delamerian Orogen. *Geological Society, London, Special Publications*, *413*(1), 269–299. https://doi.org/10.1144/SP413.8

Gibson, G. M., & Ireland, T. R. (1996). Extension of delamerian (Ross) orogen into western New Zealand: Evidence from zircon ages and implications for crustal growth along the Pacific margin of Gondwana. *Geology*, *24*(12), 1087–1090. https://doi.org/10.1130/0091-7613(1996)024%3C1087:EODROI%3E2.3.CO;2

Goodge, J. W., & Fanning, C. M. (2016). Mesoarchean and Paleoproterozoic history of the Nimrod Complex, central Transantarctic Mountains, Antarctica: Stratigraphic revisions and relation to the Mawson Continent in east Gondwana. *Precambrian Research*, *285*, 242–271. https://doi.org/10.1016/j.precamres.2016.09.001

Goodge, J. W., Mark Fanning, C., Norman, M. D., & Bennett, V. C. (2012). Temporal, isotopic and spatial relations of early paleozoic Gondwana-margin arc magmatism, central Transantarctic Mountains, Antarctica. *Journal of Petrology*, *53*(10), 2027–2065. https://doi.org/10.1093/petrology/egs043

Grimes, C. B., Wooden, J. L., Cheadle, M. J., & John, B. E. (2015). "Fingerprinting" tectono-magmatic provenance using trace elements in igneous zircon. *Contributions to Mineralogy and Petrology*, *170*(5-6), 46. https://doi.org/10.1007/s00410-015-1199-3

Grunow, A. M., Kent, D. V., & Dalziel, I. W. D. (1987). Mesozoic evolution of West Antarctica and the Weddell Sea basin: New paleomagnetic constraints. *Earth and Planetary Science Letters*, *86*(1), 16–26. https://doi.org/10.1016/0012-821X(87)90184-1

Gunn, B. M., & Warren, G. (1962). Geology of Victoria Land between the Mawson and Mullock Glaciers, Antarctica. *New Zealand Geological Survey Bulletin*, *71*, 157. Retrieved from http://trove.nla.gov.au/work/21285143?selectedversion=NBD2636400, accessed March 2017.

Hagen-Peter, G., & Cottle, J. (2017). Evaluating the relative roles of crustal growth versus reworking through continental arc magmatism: A case study from the Ross orogen, Antarctica. *Gondwana Research*. https://doi.org/10.1016/j.gr.2017.11.006

Hagen-Peter, G., Cottle, J. M., Tulloch, A. J., & Cox, S. C. (2015). Mixing between enriched lithospheric mantle and crustal components in a short-lived subduction-related magma system, Dry Valleys area, Antarctica: Insights from U-Pb geochronology, Hf isotopes, and whole-rock geochemistry. *Lithosphere*, *7*(2), 174–188. https://doi.org/10.1130/L384.1

Hervé, F., Fanning, C. M., Calderón, M., & Mpodozis, C. (2014). Early Permian to Late Triassic batholiths of the Chilean frontal cordillera (28°-31°S): SHRIMP U-Pb zircon ages and Lu-Hf and O isotope systematics. *Lithos*, *184-187*, 436–446. https://doi.org/10.1016/j.lithos.2013.10.018

Hiess, J., Yi, K., Woodhead, J., Ireland, T., & Rattenbury, M. (2015). Gondwana margin evolution from zircon REE, O and Hf signatures of Western Province gneisses, Zealandia. *Geological Society, London, Special Publications*, *389*(1), 323–353. https://doi.org/10.1144/SP389.10

Hinkley, T. K., Smith, K. S., Taggart, J. E., & Brown, J. T. (1980). Chemical and mineralogical aspects of the observed fractionation of ash from the May 18, 1980 eruption of Mount St. Helens. *U.S. Geological Survey Professional Paper*, *1397–A*, 73. https://pubs.usgs.gov/pp/1397/report.pdf (accessed March 2017).

Hoskin, P. W. O., & Ireland, T. R. (2000). Rare earth element chemistry of zircon and its use as a provenance indicator. *Geology*, *28*(7), 627. https://doi.org/10.1130/0091-7613(2000)28%3C627:REECOZ%3E2.0.CO;2

Jackson, S. E., Pearson, N. J., Griffin, W. L., & Belousova, E. A. (2004). The application of laser ablation-inductively coupled plasma-mass spectrometry to in situ U–Pb zircon geochronology. *Chemical Geology*, *211*(1-2), 47–69. https://doi.org/10.1016/j.chemgeo.2004.06.017

Jeon, H., Williams, I. S., & Bennett, V. C. (2014). Uncoupled O and Hf isotopic systems in zircon from the contrasting granite suites of the New England Orogen, eastern Australia: Implications for studies of Phanerozoic magma genesis. *Geochimica et Cosmochimica Acta*, *146*, 132–149. https://doi.org/10.1016/j.gca.2014.09.042

Kemp, A. I. S., Hawkesworth, C. J., Collins, W. J., Gray, C. M., & Blevin, P. L. (2009). Isotopic evidence for rapid continental growth in an extensional accretionary orogen: The Tasmanides, eastern Australia. *Earth and Planetary Science Letters*, *284*(3-4), 455–466. https://doi.org/10.1016/j.epsl.2009.05.011

Kemp, A. I. S., Hawkesworth, C. J., Foster, G. L., Paterson, B. A., Woodhead, J. D., Hergt, J. M., … Whitehouse, M. J. (2007). Magmatic and crustal differentiation history of granitic rocks from Hf-O isotopes in zircon. *Science*, 315. http://science.sciencemag.org/content/315/5814/980 (accessed March 2017).

Kemp, A. I. S., Wormald, R. J., Whitehouse, M. J., & Price, R. C. (2005). Hf isotopes in zircon reveal contrasting sources and crystallization histories for alkaline to peralkaline granites of Temora, southeastern Australia. *Geology*, *33*(10), 797. https://doi.org/10.1130/G21706.1

Kimbrough, D. L., Tulloch, A. J., Coombs, D. S., Landis, C. A., Johnston, M. R., & Mattinson, J. M. (1994). Uranium lead zircon ages from the Median Tectonic Zone, New Zealand. *New Zealand Journal of Geology and Geophysics*, *37*(4), 393–419. https://doi.org/10.1080/00288306.1994.9514630

Kylander-Clark, A. R. C., Hacker, B. R., & Cottle, J. M. (2013). Laser-ablation split-stream ICP petrochronology. *Chemical Geology*, *345*, 99–112. https://doi.org/10.1016/j.chemgeo.2013.02.019

Lawver, L. A., Dalziel, I. W. D., Norton, I. O., Gahagan, L. M., & Davis, J. (2014). The PLATES 2013 atlas of plate reconstructions (550 Ma to present day): PLATES Progress Report No. 367–0214, University, p. 212.

LeMasurier, W. E., & Landis, C. A. (1996). Mantle-plume activity recorded by low-relief erosion surfaces in West Antarctica and New Zealand. *Geological Society of America Bulletin*, *108*(11), 1450–1466. https://doi.org/10.1130/0016-7606(1996)108%3C1450:MPARBL%3E2.3.CO;2

Li, P., Rosenbaum, G., Yang, J.-H., & Hoy, D. (2015). Australian-derived detrital zircons in the Permian-Triassic Gympie terrane (eastern Australia): Evidence for an autochthonous origin. *Tectonics*, *34*(5), 858–874. https://doi.org/10.1002/2015TC003829

Liu, Y., Hu, Z., Zong, K., Gao, C., Gao, S., Xu, J., & Chen, H. (2010). Reappraisement and refinement of zircon U-Pb isotope and trace element analyses by LA-ICP-MS. *Chinese Science Bulletin*, *55*(15), 1535–1546. https://doi.org/10.1007/s11434-010-3052-4

Ludwig, K. R. (2003). *User's manual for Isoplot/EX, version 3.0, a geochronological toolkit for Microsoft Excel*, *Berkeley Geochronology Center Special Publication* (Vol. 4). Retrieved from https://searchworks.stanford.edu/view/6739593, accessed March 2017.

McKay, M. P., Coble, M. A., Hessler, A. M., Weislogel, A. L., & Fildani, A. (2016). Petrogenesis and provenance of distal volcanic tuffs from the Permian-Triassic Karoo Basin, South Africa: A window into a dissected magmatic province. *Geosphere*, *12*(1), 1–14. https://doi.org/10.1130/GES01215.1

McKinney, S. T., Cottle, J. M., & Lederer, G. W. (2015). Evaluating rare earth element (REE) mineralization mechanisms in Proterozoic gneiss, Music Valley, California. *Geological Society of America Bulletin*, *127*, B31165.1. https://doi.org/10.1130/B31165.1

Meert, J. G., & Lieberman, B. S. (2008). The Neoproterozoic assembly of Gondwana and its relationship to the Ediacaran–Cambrian radiation. *Gondwana Research*, *14*(1-2), 5–21. https://doi.org/10.1016/j.gr.2007.06.007

Milan, L. A., Daczko, N. R., Clarke, G. L., & Allibone, A. H. (2016). Complexity of in-situ zircon U–Pb–Hf isotope systematics during arc magma genesis at the roots of a Cretaceous arc, Fiordland, New Zealand. *Lithos*, *264*, 296–314. https://doi.org/10.1016/j.lithos.2016.08.023

Millar, I. L., Pankhurst, R. J., & Fanning, C. M. (2002). Basement chronology of the Antarctic Peninsula: Recurrent magmatism and anatexis in the Palaeozoic Gondwana margin. *Journal of the Geological Society*, *159*(2), 145–157. https://doi.org/10.1144/0016-764901-020

Mortimer, N., Gans, P., Calvert, A., & Walker, N. (1999). Geology and thermochronometry of the east edge of the Median Batholith (Median Tectonic Zone): A new perspective on Permian to Cretaceous crustal growth of New Zealand. *Island Arc*, *8*(3), 404–425. https://doi.org/10.1046/j.1440-1738.1999.00249.x

Mortimer, N., Rattenbury, M., King, P., Bland, K., Barrell, D., Bache, F., … Turnbull, R. E. (2014). High-level stratigraphic scheme for New Zealand rocks. *New Zealand Journal of Geology and Geophysics*, *57*(4), 402–419. https://doi.org/10.1080/00288306.2014.946062

Mortimer, N., Turnbull, R. E., Palin, J. M., Tulloch, A. J., Rollet, N., & Hashimoto, T. (2015). Triassic–Jurassic granites on the Lord Howe Rise, northern Zealandia. *Australian Journal of Earth Sciences*, *99*, 1–8. https://doi.org/10.1080/08120099.2015.1081984

Mukasa, S. B., & Dalziel, I. W. D. (2000). Marie Byrd Land, West Antarctica: Evolution of Gondwana's Pacific margin constrained by zircon U-Pb geochronology and feldspar common-Pb isotopic compositions. *Bulletin of the Geological Society of America*, *112*(4), 611–627. https://doi.org/10.1130/0016-7606(2000)112%3C611:MBLWAE%3E2.0.CO;2

Murgulov, V., Beyer, E., Griffin, W. L., O'Reilly, S. Y., Walters, S. G., & Stephens, D. (2007). Crustal evolution in the Georgetown Inlier, North Queensland, Australia: A detrital zircon grain study. *Chemical Geology*, *245*(3-4), 198–218. https://doi.org/10.1016/j.chemgeo.2007.08.001

Nebel, O., Münker, C., Nebel-Jacobsen, Y. J., Kleine, T., Mezger, K., & Mortimer, N. (2007). Hf–Nd–Pb isotope evidence from Permian arc rocks for the long-term presence of the Indian–Pacific mantle boundary in the SW Pacific. *Earth and Planetary Science Letters*, *254*(3-4), 377–392. https://doi.org/10.1016/j.epsl.2006.11.046

Pankhurst, R., & Weaver, S. (1998). Geochronology and geochemistry of pre-Jurassic superterranes in Marie Byrd Land, Antarctica. *Journal of Geophysical Research*, *103*(B2), 2529–2547. https://doi.org/10.1029/97JB02605

Pankhurst, R. J., Hervé, F., Fanning, C. M., Calderón, M., Niemeyer, H., Griem-Klee, S., & Soto, F. (2016). The pre-Mesozoic rocks of northern Chile: U–Pb ages, and Hf and O isotopes. *Earth-Science Reviews*, *152*, 88–105. https://doi.org/10.1016/j.earscirev.2015.11.009

Pankhurst, R. J., Millar, I. L., Grunow, A. M., & Storey, B. C. (1993). The pre-Cenozoic magmatic history of the Thurston Island crustal block, West Antarctica. *Journal of Geophysical Research*, *98*(B7), 11,835–11,849. https://doi.org/10.1029/93JB01157

Patchett, P. J., & Tatsumoto, M. (1980). Hafnium isotope variations in oceanic basalts. *Geophysical Research Letters*, *7*(12), 1077–1080. https://doi.org/10.1029/GL007i012p01077

Patchett, P. J., & Tatsumoto, M. (1981). A routine high-precision method for Lu-Hf isotope geochemistry and chronology. *Contributions to Mineralogy and Petrology*, *75*(3), 263–267. https://doi.org/10.1007/BF01166766

Paterson, S. R., & Ducea, M. N. (2015). Arc magmatic tempos: Gathering the evidence. *Elements*, *11*(2), 91–98. https://doi.org/10.2113/gselements.11.2.91

Paton, C., Hellstrom, J., Paul, B., Woodhead, J., & Hergt, J. (2011). Iolite: Freeware for the visualisation and processing of mass spectrometric data. *Journal of Analytical Atomic Spectrometry*, *26*(12), 2508. https://doi.org/10.1039/c1ja10172b

Paton, C., Woodhead, J. D., Hellstrom, J. C., Hergt, J. M., Greig, A., & Maas, R. (2010). Improved laser ablation U-Pb zircon geochronology through robust downhole fractionation correction. *Geochemistry, Geophysics, Geosystems*, *11*(3), Q0AA06. https://doi.org/10.1029/2009GC002618

Paulsen, T. S., Encarnación, J., Grunow, A. M., Valencia, V. A., Pecha, M., Layer, P. W., & Rasoazanamparany, C. (2013). Age and significance of "outboard" high-grade metamorphics and intrusives of the Ross orogen, Antarctica. *Gondwana Research*, *24*(1), 349–358. https://doi.org/10.1016/j.gr.2012.10.004

Pepper, M., Gehrels, G., Pullen, A., Ibanez-Mejia, M., Ward, K. M., & Kapp, P. (2016). Magmatic history and crustal genesis of western South America: Constraints from U-Pb ages and Hf isotopes of detrital zircons in modern rivers. *Geosphere*, *12*(5), 1532–1555. https://doi.org/10.1130/GES01315.1

Phillips, G., Landenberger, B., & Belousova, E. A. (2011). Building the New England Batholith, eastern Australia—Linking granite petrogenesis with geodynamic setting using Hf isotopes in zircon. *Lithos*, *122*(1-2), 1–12. https://doi.org/10.1016/j.lithos.2010.11.005

Regmi, K. R., Weinberg, R. F., Nicholls, I. A., Maas, R., & Raveggi, M. (2016). Evidence for hybridisation in the Tynong Province granitoids, Lachlan Fold Belt, eastern Australia. *Australian Journal of Earth Sciences*, *63*(3), 235–255. https://doi.org/10.1080/08120099.2016.1180321

Rey, A., Deckart, K., Arriagada, C., & Martínez, F. (2016). Resolving the paradigm of the late Paleozoic–Triassic Chilean magmatism: Isotopic approach. *Gondwana Research*, *37*, 172–181. https://doi.org/10.1016/j.gr.2016.06.008

Riley, T. R., Flowerdew, M. J., Pankhurst, R. J., Leat, P. T., Millar, I. L., Fanning, C. M., & Whitehouse, M. J. (2017). A revised geochronology of Thurston Island, West Antarctica, and correlations along the proto-Pacific margin of Gondwana. *Antartic Science*, *29*(01), 47–60. https://doi.org/10.1017/S0954102016000341

Rubatto, D. (2002). Zircon trace element geochemistry: Partitioning with garnet and the link between U–Pb ages and metamorphism. *Chemical Geology*, *184*(1-2), 123–138. https://doi.org/10.1016/S0009-2541(01)00355-2

Rudnick, R. L., & Gao, S. (2003). Composition of the continental crust. *Treatise on Geochemistry*, *3*, 659.

Schöner, R., Viereck-Goette, L., Schneider, J., & Bomfleur, B. (2007). Triassic-Jurassic sediments and multiple volcanic events in north Victoria Land, Antarctica: A revised stratigraphy. In A. K. Cooper, et al. (Eds.), *Antarctica: A keystone in a changing world. Online proceedings of the 10th ISAES, USGS Open-File Report 2007-1047, Short Research Paper 102* (5 p.). https://doi.org/10.3133/of2007-1047.srp102

Scott, J. M., Cooper, A. F., Palin, J. M., Tulloch, A. J., Kula, J., Jongens, R., … Pearson, N. J. (2009). Tracking the influence of a continental margin on growth of a magmatic arc, Fiordland, New Zealand, using thermobarometry, thermochronology, and zircon U-Pb and Hf isotopes. *Tectonics*, *28*(6), p. TC6007. https://doi.org/10.1029/2009TC002489

Scott, J. M., Palin, J. M., Cooper, A. F., Sagar, M. W., Allibone, A. H., & Tulloch, A. J. (2011). From richer to poorer: Zircon inheritance in Pomona Island Granite, New Zealand. *Contributions to Mineralogy and Petrology*, *161*(5), 667–681. https://doi.org/10.1007/s00410-010-0556-5

Shaanan, U., Rosenbaum, G., & Wormald, R. (2015). Provenance of the Early Permian Nambucca Block (eastern Australia) and implications for the role of trench retreat in accretionary orogens. *Geological Society of America Bulletin*, *127*, B31178.1. https://doi.org/10.1130/B31178.1

Shaw, S. E., Flood, R. H., & Pearson, N. J. (2011). The New England Batholith of eastern Australia: Evidence of silicic magma mixing from zircon $^{176}Hf/^{177}Hf$ ratios. *Lithos*, *126*(1-2), 115–126. https://doi.org/10.1016/j.lithos.2011.06.011

Sláma, J., Košler, J., Condon, D. J., Crowley, J. L., Gerdes, A., Hanchar, J. M., … Whitehouse, M. J. (2008). Plešovice zircon—A new natural reference material for U–Pb and Hf isotopic microanalysis. *Chemical Geology*, *249*(1-2), 1–35. https://doi.org/10.1016/j.chemgeo.2007.11.005

Storey, B., Dalziel, I. W., Garrett, S., Grunow, A., Pankhurst, R., & Vennum, W. (1988). West Antarctica in Gondwanaland: Crustal blocks, reconstruction and breakup processes. *Tectonophysics*, *155*(1-4), 381–390. https://doi.org/10.1016/0040-1951(88)90276-4

Taylor, H. E., & Lichte, F. E. (1980). Chemical composition of Mount St. Helens volcanic ash. *Geophysical Research Letters*, *7*(11), 949–952. https://doi.org/10.1029/GL007i011p00949

Thirlwall, M. F., & Anczkiewicz, R. (2004). Multidynamic isotope ratio analysis using MC–ICP–MS and the causes of secular drift in Hf, Nd and Pb isotope ratios. *International Journal of Mass Spectrometry*, *235*(1), 59–81. https://doi.org/10.1016/j.ijms.2004.04.002

Tulloch, A. J., Ramezani, J., Kimbrough, D. L., Faure, K., & Allibone, A. H. (2009). U-Pb geochronology of mid-Paleozoic plutonism in western New Zealand: Implications for S-type granite generation and growth of the east Gondwana margin. *Geological Society of America Bulletin*, *121*(9-10), 1236–1261. https://doi.org/10.1130/B26272.1

Veevers, J. J., Belousova, E. A., Saeed, A., Sircombe, K., Cooper, A. F., & Read, S. E. (2006). Pan-Gondwanaland detrital zircons from Australia analysed for Hf-isotopes and trace elements reflect an ice-covered Antarctic provenance of 700–500 Ma age, TDM of 2.0–1.0 Ga, and alkaline affinity. *Earth-Science Reviews*, *76*(3-4), 135–174. https://doi.org/10.1016/j.earscirev.2005.11.001

Vermeesch, P. (2012). On the visualisation of detrital age distributions. *Chemical Geology*, *312-313*, 190–194. https://doi.org/10.1016/j.chemgeo.2012.04.021

Vervoort, J. D., & Blichert-Toft, J. (1999). Evolution of the depleted mantle: Hf isotope evidence from juvenile rocks through time. *Geochimica et Cosmochimica Acta*, *63*(3-4), 533–556. https://doi.org/10.1016/S0016-7037(98)00274-9

Walker, J. D., Geissman, J. W., Bowring, S. A., & Babcock, L. E. (2013). The Geological Society of America geologic time scale. *Geological Society of America Bulletin*, *125*(3-4), 259–272. https://doi.org/10.1130/B30712.1

Wiedenbeck, M., Alle, P., Corfu, F., Griffin, W. L., Meier, M., Oberli, F., … Spiegel, W. (1995). Three natural zircon standards for U-Th-Pb, Lu-Hf, trace element and REE analyses. *Geostandards and Geoanalytical Research*, *19*(1), 1–23. https://doi.org/10.1111/j.1751-908X.1995.tb00147.x

Wiedenbeck, M., Hanchar, J. M., Peck, W. H., Sylvester, P., Valley, J., Whitehouse, M., … Zheng, Y. F. (2004). Further characterisation of the 91500 zircon crystal. *Geostandards and Geoanalytical Research*, *28*(1), 9–39. https://doi.org/10.1111/j.1751-908X.2004.tb01041.x

Woodhead, J. D., & Hergt, J. M. (2005). A preliminary appraisal of seven natural zircon reference materials for in situ Hf isotope determination. *Geostandards and Geoanalytical Research*, *29*(2), 183–195. https://doi.org/10.1111/j.1751-908X.2005.tb00891.x

Yakymchuk, C., Brown, C. R., Brown, M., Siddoway, C. S., Fanning, C. M., & Korhonen, F. J. (2015). Paleozoic evolution of western Marie Byrd Land, Antarctica. *Bulletin of the Geological Society of America*, *127*(9-10), 1464–1484. https://doi.org/10.1130/B31136.1

## Erratum

In the originally published version of this article, Figure 6 had two typos. $^{176}Lu/^{177}H$ should read $^{176}Lu/^{177}Hf$. Also, "recycling" was misspelled twice. The typos have since been corrected, and this version may be considered the authoritative version of record.